

TUTORIAL REVIEW



Cite this: *Chem. Soc. Rev.*, 2025, 54, 3247

Biocatalytic cascade reactions for management of diseases

Ya-Ping Xiao,^{ac} Jiayingzi Wu,^a Peng-Hang Chen,^a Shan Lei,^a Jing Lin,^{id} ^{*a}
Xin Zhou^{id} ^{*bd} and Peng Huang^{id} ^{*a}

Biocatalytic cascade reactions, which evolve from the confinement of multiple enzymes within living cells, represent a promising strategy for disease management. Using tailor-made nanoplateforms, reactions induced by multiple enzymes and/or nanozymes can be precisely triggered at pathogenic sites. These promote further cascade reactions that generate therapeutic species prompting effective therapeutic outcomes with minimal side effects. Over the past few years, this approach has seen widespread applications in disease management. This review attempts to critically assess and summarize the recent advances in the use of biocatalytic cascade reactions for the management of diseases. Emphasis is placed on the design of cascade catalytic systems of high efficiency and selectivity and the implementation of specific cascade processes that respond to the endogenous substances produced in the pathological processes. The various types of biocatalytic cascade reactions are outlined according to the timeline of the catalytic steps through a series of reported examples. The challenges and outlook in the field are also discussed to encourage the further development of personalized treatments based on biocatalytic cascade reactions.

Received 29th August 2024

DOI: 10.1039/d3cs00410d

rsc.li/chem-soc-rev

Key learning points

1. The concepts and advantages of biocatalytic cascade reactions.
2. Innovative ideas for biocatalytic cascade reactions applicable to disease treatment.
3. A deep understanding of the catalytic mechanisms of different types of biocatalytic cascade reactions.
4. Notable examples from the literature that highlight various biocatalytic cascade reactions used for specific disease treatment.
5. Key challenges and outlook on the further development of biocatalytic cascade reactions in disease management.

1. Introduction

Biocatalysis, the application of enzymes to solve problems in synthetic chemistry, has become a powerful technology for chemical innovation.¹ Compared to traditional avenues of chemical syntheses, which usually require the success of multistep

reactions under strictly defined conditions (temperature, pH, solvents, catalysts, substrates, *etc.*) to achieve a high yield, biological catalysis can rapidly reach a maximum yield in aqueous solutions at neutral pH and mild temperature. With the inherent efficiency and selectivity of enzymes, biocatalysis can avoid cross-reactivity between substrates and unwanted by-products and reduce the number of steps required for synthesis.² Additionally, enzymes are biocompatible and biodegradable, thus biocatalysis can avoid or at least reduce the use of toxic reagents and solvents. As such, biocatalysis is regarded as a practical and environmentally friendly alternative to traditional metallo- and organo-catalysis, exhibiting appealing prospects for biomedical applications.

Biological cascade catalysis reactions mediated by multiple enzymes drive efficient, selective, and complex intracellular biocatalytic transformations in living organisms.³ In biological cascade reactions, at least two enzymatic reactions are carried out, and the product generated from the first enzymatic reaction serves as the substrate for the second. Inspired by nature,

^a Marshall Laboratory of Biomedical Engineering, International Cancer Center, Guangdong Key Laboratory for Biomedical Measurements and Ultrasound Imaging, Laboratory of Evolutionary Theranostics (LET), School of Biomedical Engineering, Shenzhen University Medical School, Shenzhen University, Shenzhen, 518055, China. E-mail: peng.huang@szu.edu.cn, jingl@szu.edu.cn

^b State Key Laboratory of Magnetic Resonance Spectroscopy and Imaging, Wuhan Institute of Physics and Mathematics, Innovation Academy for Precision Measurement Science and Technology, Chinese Academy of Sciences, Wuhan, 430071, China. E-mail: xinzhou@wipm.ac.cn

^c School of Life and Health Technology, Dongguan University of Technology, Dongguan, 523808, China

^d School of Biomedical Engineering, Hainan University, Haikou, 570228, China

biological cascade reactions have been used to combine several catalytic steps in one pot to produce a wide range of chemical commodities. By avoiding the intermediates' isolation and purification steps, biological cascade catalysis improves the atom economy of the overall process, providing a time-saving and lower-cost alternative to multistep reactions. Benefiting from the enhanced local concentration of intermediates, biological cascade reactions exhibit superior performances, such as improved catalytic efficiency, by improving the utilization of unstable intermediates and increasing the signal intensity. In addition, the problem of toxic intermediate(s) can be solved in cascade reactions. Inspired by these merits, great efforts have been made to develop novel cascade catalytic systems that mimic biological cascade reactions in the past few years.

Catalysis and medicine are two independent research fields that have developed rapidly but independently, until the last decade, when some nanocatalysts, such as nanozymes, photocatalysts, and electrocatalysts, were employed to induce catalytic reactions *in vivo* to realize therapeutic effects. With the rapid development of nanocatalysts in biomedical applications, the gradual integration of nanocatalysis within nanomedicine has promoted the emergence of nanocatalytic therapies.⁴ Among the various known nanocatalysts, nanozymes, a type of nanomaterial with enzyme-like catalytic properties, have attracted increasing interest due to their intrinsic merits of low cost, high and tunable catalytic stability, easy preparation, and good storage stability.⁵ As such, nanozymes can not only overcome the intrinsic deficiencies of natural enzymes, such as their high cost, low operational stability, short shelf-life, and requirement



Ya-Ping Xiao

materials for therapy and theranostics.

Ya-Ping Xiao is an Associate Researcher at the School of Life and Health Technology, Dongguan University of Technology, China. She received her PhD in Organic Chemistry from the Sichuan University in 2020. She then joined the Laboratory of Evolutionary Theranostics (LET) at the Shenzhen University as a postdoctoral fellow. She is currently an Associate Researcher at Dongguan University of Technology. Her research focuses on the development of smart nano-



Jing Lin

Shenzhen University (SZU) in 2016 and was promoted as a Distinguished Professor in 2018. Her research focuses on molecular imaging, nanomedicine and theranostics.

Jing Lin is a Distinguished Professor at the School of Biomedical Engineering, Shenzhen University Medical School, China. She received her PhD in Organic Chemistry from the Donghua University and Shanghai Institute of Organic Chemistry, Chinese Academy of Sciences in 2010. After two years, she moved to the United States of America and spent 4 years as a postdoc at the University of Maryland and the National Institutes of Health (NIH). She joined the faculty of



Xin Zhou

lung hyperpolarized gas magnetic resonance imaging (MRI), which was the first clinically approved xenon polarizer and multi-nuclear MRI instrument in China. Additionally, he has made significant contributions in the field of MRI new technologies and high-sensitivity molecular imaging.

Xin Zhou, Professor and President of the Innovation Academy for Precision Measurement Science and Technology (APM), Chinese Academy of Sciences (CAS). He holds a PhD from the Graduate School of CAS, and subsequently engaged in postdoctoral research at Harvard Medical School followed by a research fellow position at the college of chemistry, UC Berkeley. In 2009, he joined the APM, as a full professor. Prof. Zhou pioneered



Peng Huang

as a postdoctoral fellow. In 2015, he moved to Shenzhen University as a Distinguished Professor. His research focuses on molecular imaging, nanomedicine and theranostics.

Peng Huang is a Distinguished Professor, Chief of the Laboratory of Evolutionary Theranostics (LET), and Director of the Department of Molecular Imaging, at the School of Biomedical Engineering, Shenzhen University Medical School, China. He received his PhD degree in Biomedical Engineering from the Shanghai Jiao Tong University in 2012. He then joined the Laboratory of Molecular Imaging and Nanomedicine (LOMIN) at the National Institutes of Health (NIH)

for mild catalytic conditions, but also provide an extremely promising opportunity to develop novel biomimetic cascade nanoreactors. For example, a nanozyme can be used to replace one enzyme of a multi-enzyme cascade catalytic system to construct enzyme–nanozyme hybrid cascade nanoreactors. Additionally, nanozymes can act as carriers for natural enzymes and further improve the efficiency and stability of hybrid cascade catalytic systems by facilitating the transformation of intermediates from one enzyme to another enzyme/nanozyme.⁶ In addition, nanozyme–enzyme cascade nanoreactors, which use nanozymes to replace the natural enzymes in cascade catalytic systems, also exhibit higher catalytic stability and efficiency due to the high catalytic stability and tunable catalytic activity of nanozymes. Furthermore, nanozyme-engineered biomimetic cascade nanoreactors can employ endogenous substrates (glucose, lactate, H_2O_2 , etc.) to initiate cascade reactions for the management of various diseases, including but not limited to cancer, neurodegenerative diseases, and wound infections, significantly promoting the application of biocatalytic cascade reactions for disease treatment.

Enzyme- and/or nanozyme-engineered biomimetic cascade catalytic nanoreactors have been extensively studied, and impressive progress has been achieved in the construction of cascade catalytic systems for disease treatment. However, previous reviews have either focused on the use of natural enzyme-induced cascade reactions for the preparation of organic molecules or nanozyme-engineered biomimetic cascade reactions to demonstrate how biocatalytic cascade reactions can be used in biomedical applications, including but not limited to disease treatment.

Herein, we highlight the recent progress toward understanding the mechanisms of cascade catalysis and the efficient treatment of diseases using enzyme- and/or nanozyme-engineered biocatalytic

cascade reactions. We first summarize and categorize the enzyme- and/or nanozyme-engineered biocatalytic cascade reactions according to the timeline of the catalytic steps (*i.e.*, linear cascade, orthogonal cascade, parallel cascade, and cyclic cascade, *etc.*).⁷ Subsequently, the applications of enzyme- and/or nanozyme-derived biocatalytic cascade systems in the management of various diseases, including cancer, oxidative stress-related diseases, wound infection, and hyperuricemia are explored in detail (Fig. 1). Finally, the challenges involved and prospects for the further development of biocatalytic cascade systems as therapeutics are discussed. This review aims to provide a navigation tool for those interested in the design of enzymes and/or nanozyme-induced biocatalytic cascade reactions for disease management, paving the way for new disease therapies or theranostics.

2. Categories of biocatalytic cascade reactions

A large number of biocatalytic cascade reactions based on different enzymes and/or nanozymes with high catalytic activity and good specificity have been established for disease management in the past few decades (Table 1). According to the timeline of catalytic steps, biocatalytic cascade reactions are classified into five main categories: linear, orthogonal, parallel, cyclic, and triangular cascades (Fig. 2).⁷

2.1 Linear cascades

As the most common and straightforward approach, linear cascades apply consecutive reactions to convert a single substrate into a single product in a multi-step one-pot manner. The unique characteristics of linear cascades can not only rapidly transform unstable or toxic intermediates, but also reduce side reactions and improve yields, thus linear cascades are regarded as safe processes. Various linear cascades driven by enzymes and/or nanozymes have been reported for use in biomedical applications. One commonly applied linear cascade is the superoxide dismutase-catalase (SOD-CAT) system, in which SOD or SOD-like nanozymes transform the superoxide anion ($\text{O}_2^{\bullet-}$) into H_2O_2 . The generated H_2O_2 is catalyzed by CAT or CAT-like nanozymes to produce H_2O and O_2 . Qu and colleagues successfully prepared a SOD-CAT cascade system by doping hydrogen-bonded organic framework (HOF) shells with porous carbon nanosphere nanozymes (PCNs) for encapsulating neural stem cells (NSC@PCN/HOF) (Fig. 3A).⁸ Through the SOD- and CAT-like activities of PCNs, NSC@PCN/HOF converts $\text{O}_2^{\bullet-}$ into H_2O_2 , which is subsequently decomposed into O_2 . In the presence of L-arginine, the O_2 generated by the SOD-CAT cascade can act as the substrate for the nitric oxide synthase (iNOS) to generate NO through the manner of SOD-CAT-iNOS cascade (Fig. 3B).⁹ Additionally, H_2O_2 can also be used as the substrate for glutathione peroxidase (GPx) or GPx-like nanozymes, lactoperoxidase (LPO) or LPO-like nanozymes, and peroxidase (POD) or POD-like nanozymes. For example, Zhang and colleagues reported their formulation of an oligomeric semiconducting nanozyme that can catalyze $\text{O}_2^{\bullet-}$ into H_2O_2

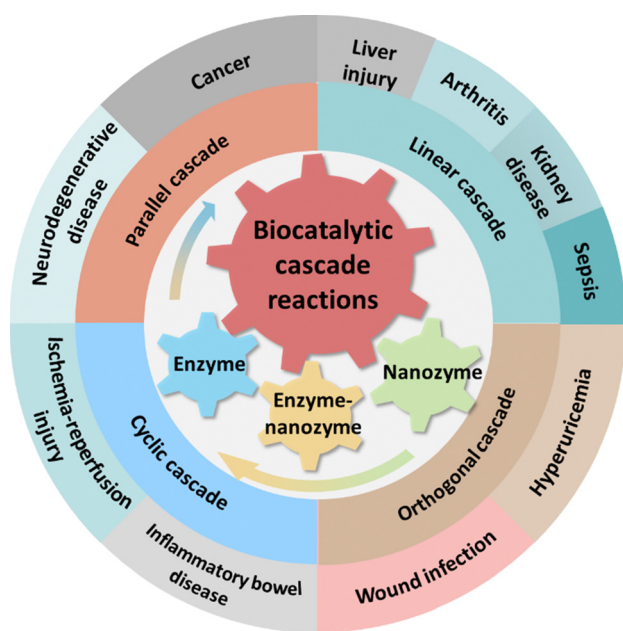


Fig. 1 Overview of biocatalytic cascade reactions used in the management of diseases, with emphasis on various types of biocatalytic cascade reactions.

Table 1 Summary of representative types of biocatalytic cascade reactions used in disease treatment

Classification	Cascade catalytic system	Enzyme/enzyme mimic	Reaction process	Ref.
Linear cascades	NCS@PCN/HOF	SOD, CAT	$O_2^{\bullet-} \xrightarrow{SOD} H_2O_2 \xrightarrow{CAT} O_2$	8
	Pt-iNOS@ZIF	SOD, CAT, iNOS	$O_2^{\bullet-} \xrightarrow{SOD} H_2O_2 \xrightarrow{CAT} O_2 \xrightarrow{iNOS} NO$	9
	O-NZ	SOD, GPx	$O_2^{\bullet-} \xrightarrow{SOD} H_2O_2 \xrightarrow{GPx} H_2O$	10
	E-I-P-SNs	SOD, LPO	$O_2^{\bullet-} \xrightarrow{SOD} H_2O_2 \xrightarrow{LPO} {}^1O_2$	11
	COF-909-M	SOD, POD, GPx	$O_2^{\bullet-} \xrightarrow{SOD} H_2O_2 \xrightarrow{POD} \bullet OH$	12
	Liposome-TiN-GOx-pH-PEG	POD, GOx	$O_2 \xrightarrow{GOx} H_2O_2 \xrightarrow{POD} \bullet OH$	13
	AuNR@Enzymes-MOF	CAT, GOx, HRP	$H_2O_2 \xrightarrow{CAT} O_2 \xrightarrow{GOx} H_2O_2 \xrightarrow{HRP} \bullet OH$	14
Orthogonal cascades	$Fe_3O_4/Ag/Bi_2MoO_6$	SOD, CAT, POD, GSHOD	$ \begin{array}{c} H_2O_2 \xrightarrow{POD} \bullet OH \\ Fe^{2+}/Mo^{5+} \xrightarrow{\bullet OH} Fe^{3+}/Mo^{6+} \\ \downarrow GSHOD \\ H_2O_2 \xrightarrow{HRP} \bullet OH \\ Fe^{2+} \xrightarrow{\bullet OH} Fe^{3+} \\ \downarrow GSHOD \end{array} $	16
	PDA/ Fe_3O_4	HRP, GSHOD	$ \begin{array}{c} H_2O_2 \xrightarrow{HRP} \bullet OH \\ Fe^{2+} \xrightarrow{\bullet OH} Fe^{3+} \\ \downarrow GSHOD \end{array} $	17
	IrO_x -GOD	POD, CAT, OXD, GOD	$ \begin{array}{c} H_2O_2 \xrightarrow{POD} \bullet OH \\ O_2 \xrightarrow{OXD} O_2^{\bullet-} \\ \downarrow GOD \end{array} $	18
Parallel cascades	$Ir-N_5$ SA	POD, CAT, OXD, NOX	$ \begin{array}{c} H_2O_2 \xrightarrow{POD} \bullet OH \\ O_2 \xrightarrow{OXD} O_2^{\bullet-} \\ \downarrow NOX \end{array} $	19
	Pd-Ru/uricase@RBC	Uricase, CAT	$ \begin{array}{c} O_2 \xrightarrow{Uricase} H_2O_2 \\ H_2O_2 \xrightarrow{CAT} O_2 \end{array} $	20
	Mn-GOx/HA	GOx, CAT	$ \begin{array}{c} O_2 \xrightarrow{GOx} H_2O_2 \\ H_2O_2 \xrightarrow{CAT} O_2 \end{array} $	21
	FPGLC	GOx, LOx, CAT	$ \begin{array}{c} H_2O_2 \xrightarrow{LOx} O_2 \\ O_2 \xrightarrow{GOx} H_2O_2 \\ \downarrow CAT \end{array} $	22
Cyclic cascades	Fe-MoOv	CAT, OXD, NOX, POD	$ \begin{array}{c} O_2 \xrightarrow{OXD} O_2^{\bullet-} \\ O_2^{\bullet-} \xrightarrow{NOX} H_2O_2 \\ H_2O_2 \xrightarrow{CAT} O_2 \end{array} $	23

via its SOD-like activity, with the H_2O_2 further transformed into H_2O through its GPx-like activity.¹⁰ Wang and colleagues prepared polyethyleneimine (PEI)-modified silica porous nano-reactors (E-I-P-SN) via the co-encapsulation of SOD, LPO, and indocyanine green.¹¹ Benefiting from the inherent characteristics of SOD and LPO, $O_2^{\bullet-}$ is first transformed into H_2O_2 by SOD, then LPO converts H_2O_2 into 1O_2 , resulting in the amplification of 1O_2 and breaking the redox balance. It is worth noting that Wang and colleagues described a series of covalent organic framework (COF)-based nanozymes with SOD-, GPx- and POD-like activities.¹² With their SOD-mimicking activity, these nanozymes catalyze a reaction with $O_2^{\bullet-}$ to produce H_2O_2 , which is then used to produce $\bullet OH$ for chemodynamic therapy (CDT). Simultaneously, the GPx-like COFs deplete glutathione (GSH) to alleviate the scavenging of H_2O_2 , synergistically enhancing the efficiency of CDT. Similarly, the glucose oxidase (GOx)-POD cascade can also amplify the generation of $\bullet OH$ for CDT.

For instance, Chun and colleagues reported an acidic-responsive NIR laser irradiation-enhanced cascade nanocatalyst (TLGp) using titanium nitride nanoparticle (TiN NP)-encapsulated liposomes linked to pH-responsive polyethylene glycol (PEG)-modified GOx.¹³ Since the GOx is covalently linked to the TLGp, TLGp can avoid the short-comings of free GOx including poor stability, short *in vivo* half-life and systemic toxicity, releasing plenty of GOx to catalyze glucose for producing abundant H_2O_2 at tumor sites after PEG detachment in acidic tumor microenvironments (TMEs), which shows enhanced tumor selectivity and reduced side effects. Subsequently, the abundant H_2O_2 is used to produce $\bullet OH$ by enhanced POD-mimicking TiN NPs, which is further improved under NIR laser irradiation owing to the good NIR-adsorption-induced surface plasmon resonance and photothermal effect. With the pH-responsive GOx-mediated H_2O_2 self-supply, nitrogen-doping, and NIR laser-enhanced enzymatic activity of TiN NPs and mild photothermal therapy, TLGp

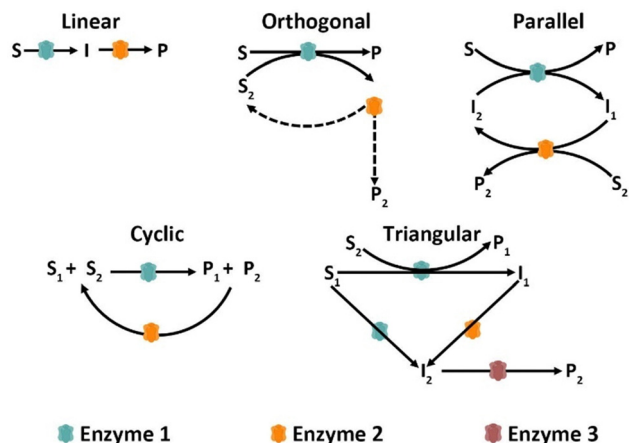


Fig. 2 Categories of biocatalytic cascade reactions according to the timeline of the catalytic steps.⁷ Reprinted (adapted) with permission from ref. 7, copyright 2020, Springer Nature.

achieves selective and cooperative tumor therapy *in vivo*. In addition, by utilizing CAT to decompose H_2O_2 into supplementary O_2 for GOx-mediated glucose oxidation, the CAT-GOx-horseradish peroxidase (HRP, POD from horseradish) cascade system effectively consumes glucose and generates $\bullet\text{OH}$ for starvation therapy and CDT, respectively (Fig. 3C).¹⁴

In general, linear cascades constructed using SOD or its mimics can quickly convert $\text{O}_2^{\bullet-}$ into H_2O_2 and O_2 with a relatively high redox potential of approximately +0.3 V.¹⁵ After introducing antioxidant enzymes, such as CAT and GPx, into SOD-engineered linear cascades, the generated H_2O_2 can be subsequently converted into H_2O and O_2 as CAT and GPx have

low redox potentials of approximately −0.1 and −0.2 V, respectively. In contrast, when oxidases, including POD, LPO, iNOS, and GOx, are added into the SOD-engineered linear cascades, these oxidases can serve as electron donors, and catalyze the production of H_2O_2 and O_2 into highly active ROS, such as $\bullet\text{OH}$, $^1\text{O}_2$, etc.

2.2 Orthogonal cascades

In orthogonal cascades, a single transformation is coupled to auxiliary enzymatic reactions to promote the formation of the desired product. Typically, orthogonal cascades used in disease treatment regenerate co-substrates to drive the equilibrium towards the desired product. However, more complex systems might be required for orthogonal cascades. For example, Dong and colleagues developed a $\text{Fe}_3\text{O}_4/\text{Ag}/\text{Bi}_2\text{MoO}_6$ nanozyme with manifold enzyme activities (mimicking POD, CAT, SOD, glutathione oxidase [GSHOD]) (Fig. 4A).¹⁶ Specifically, the prepared $\text{Fe}_3\text{O}_4/\text{Ag}/\text{Bi}_2\text{MoO}_6$ catalyzes H_2O_2 to generate $\bullet\text{OH}$ via POD-like $\text{Fe}^{2+}/\text{Mo}^{5+}$, which is regenerated by GSH depletion through the generation of GSHOD-like $\text{Fe}^{3+}/\text{Mo}^{6+}$. Similarly, the Fe_3O_4 -decorated polydopamine (PDA/ Fe_3O_4) hybrid nanozyme reported by He and colleagues also continuously produces $\bullet\text{OH}$ via $\text{Fe}^{2+}/\text{Fe}^{3+}$ redox coupling, which occurs in PDA/ Fe_3O_4 in the presence of GSH (Fig. 4B).¹⁷ Additionally, the catechol moieties of PDA can provide electrons to O_2 for generating H_2O_2 with catechol/quinone redox potentials of approximately +0.2 to +0.7 V versus a standard hydrogen electrode, further providing H_2O_2 for Fe_3O_4 to produce $\bullet\text{OH}$. Quinone groups are generated that are simultaneously reduced by GSH. With the cyclic transformation between $\text{Fe}^{2+}/\text{catechol}$ and $\text{Fe}^{3+}/\text{quinone}$, the

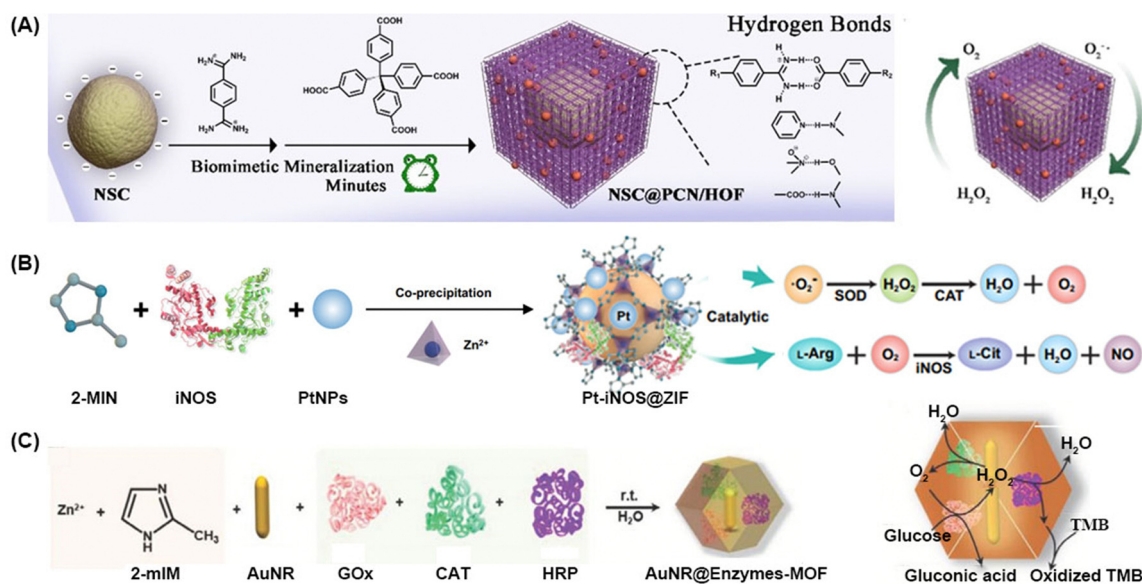


Fig. 3 Representative linear cascade reactions induced by enzymes and/or nanozymes. (A) Schematic illustration of NSC@PCN/HOF mimicking SOD-CAT cascade catalytic reactions. Reprinted (adapted) with permission from ref. 8, copyright 2022, Wiley-VCH. (B) The prepared Pt-iNOS@ZIF nanoreactor for mediating SOD-CAT-iNOS cascade reactions. Reprinted (adapted) with permission from ref. 9, copyright 2022, Springer Nature. (C) Procedure for AuNR@Enzymes-MOF synthesis consisting of an NIR-II plasmonic AuNR core and a microporous ZIF-8 MOF shell integrating CAT, GOx, and HRP (left). Schematic illustration showing the CAT-GOx-HRP cascade catalytic reactions (right). Reprinted (adapted) with permission from ref. 14, copyright 2022, Wiley-VCH.

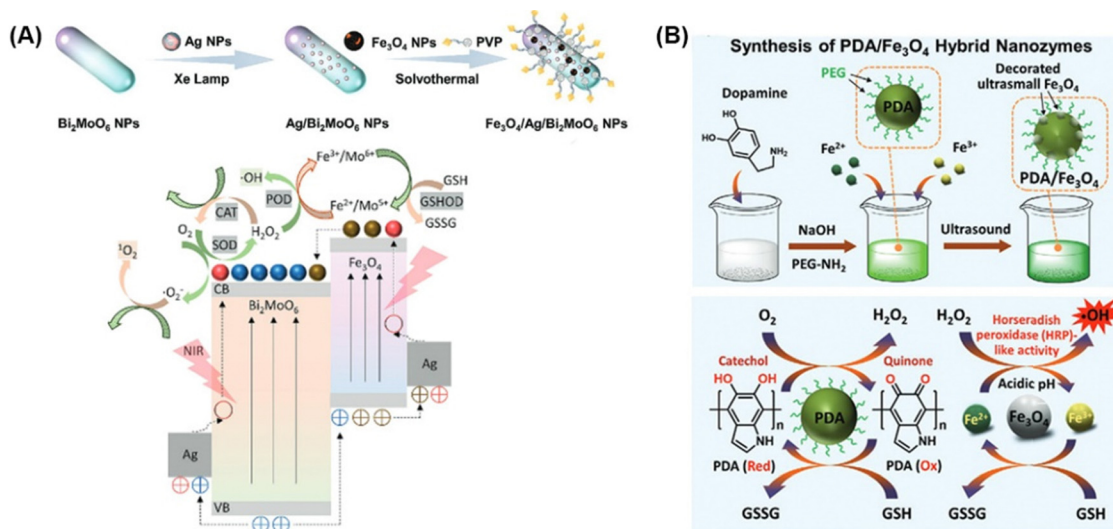


Fig. 4 Representative orthogonal cascade reactions induced by nanozymes. (A) Illustration of the cascade catalysis process induced by $\text{Fe}_3\text{O}_4/\text{Ag}/\text{Bi}_2\text{MoO}_6$ nanozyme. (B) Illustration of the prepared $\text{PDA}/\text{Fe}_3\text{O}_4$ hybrid nanozyme for continuous conversion of O_2 into •OH driven by GSH consumption. Reprinted (adapted) with permission from ref. 16, copyright 2021, Wiley-VCH and ref. 17, copyright 2022, Wiley-VCH.

$\text{PDA}/\text{Fe}_3\text{O}_4$ nanozyme enables the continuous conversion of O_2 into •OH via GSH -depleted cascade redox reactions.

2.3 Parallel cascades

In parallel cascades, two substrates are transformed into two products through two distinct biocatalytic reactions that are coupled *via* cofactors or cosubstrates. Unlike orthogonal cascades, where the by-products are discarded in most cases, the products generated in parallel cascades are considered valuable

compounds for further applications, thus parallel cascades produce substances of higher economic value. One example was reported by Jiang and colleagues, who loaded glucose oxidase (GOD) into an iridium oxide nanozyme (IrO_x) to create a hybridized nanozyme ($\text{IrO}_x\text{-GOD}$) with multienzyme mimetic activities comparable to natural CAT, POD, and oxidase (OXD) (Fig. 5A).¹⁸ With its OXD- and POD-like activities, $\text{IrO}_x\text{-GOD}$ converts O_2 and H_2O_2 into $\text{O}_2^{\bullet-}$ and •OH , respectively (Fig. 5B). The O_2 and H_2O_2 are regenerated through H_2O_2 decomposition *via* the CAT-like activity and glucose oxidation mediated by

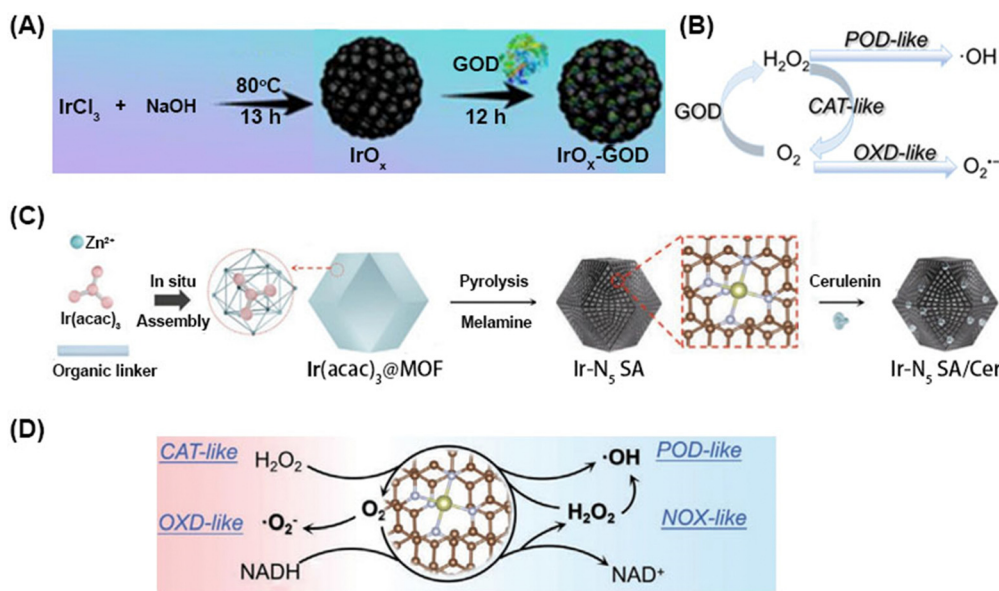


Fig. 5 Representative parallel cascade reactions induced by enzymes and/or nanozymes. Illustration of the preparation (A) and cascade catalytic process (B) of the $\text{IrO}_x\text{-GOD}$ hybrid nanozyme with multi-enzyme mimetic activities of CAT, POD, OXD and GOD. Reprinted (adapted) with permission from ref. 18, copyright 2020, Wiley-VCH. Illustration of the preparation (C) and cascade catalytic process (D) of $\text{Ir-N}_5\text{ SA/Cer}$ with OXD, POD, CAT, and NOX-like catalytic activities. Reprinted (adapted) with permission from ref. 19, copyright 2023, Wiley-VCH.

GOD. Recently, Yang and colleagues reported the generation of a novel Ir-N₅ single-atom (Ir-N₅ SA) nanozyme with OXD, POD, CAT, and nicotinamide adenine dinucleotide oxidase (NOX)-like catalytic activities (Fig. 5C).¹⁹ Ir-N₅ nanozyme can employ its CAT- and NOX-like activities to generate O₂ and H₂O₂, which promote OXD- and POD-mediated enzymatic reactions to produce O₂^{•−} and [•]OH, respectively (Fig. 5D), thereby generating massive reactive oxygen species (ROS) at the tumor sites in a H₂O₂/O₂-recyclable manner. As such, Ir-N₅ SA greatly elevates the levels of ROS, disrupting tumor redox homeostasis, which have an imbalance in the levels of ROS and antioxidants compared to normal tissues for promoting tumor growth, survival, and resistance to treatment at low to moderate levels. However, high levels of ROS can cause oxidative damage to cellular components, such as DNA, proteins, and lipids, thus leading to cancer cell death. Additionally, Ir-N₅ SA can disrupt the intracellular NADH/NAD⁺ cycle balance due to its NOX-like activity. As NADH/NAD⁺ redox pairs are electron transporters in cells, which not only provide the protons for mitochondrial electron transport chains, but are also required for adenosine triphosphate (ATP) production during tumor glycolysis and oxidative phosphorylation (OXPHOS) metabolism, thus Ir-N₅ SA can also inhibit the production of ATP through glycolysis and OXPHOS. By further cooperation with fatty acid synthase cerulenin (Cer) to inhibit fatty acid synthesis of tumor cells, the

designed Ir-N₅ SA/Cer induces significant disruption of tumor redox and metabolic homeostasis, thereby significantly enhancing the effect of tumor therapy in the 4T1 tumor-bearing mice.

2.4 Cyclic cascades

In cyclic cascades, the final product generated through the multistep cascade is transformed back into one of the starting materials. A commonly exploited benefit of cyclic cascades is the elimination of the substrates. For example, Zheng and colleagues integrated a CAT-like Pd-Ru nanozyme with uricase to reduce uric acid (UA) levels using a cyclic cascade of uricase-CAT, in which the O₂ consumed during the uricase-mediated UA degradation process is subsequently regenerated by H₂O₂ decomposition *via* the CAT-like Pd-Ru nanozyme (Fig. 6A), allowing the cascade to continue.²⁰ With the uricase-CAT cascade reactions, Pd-Ru/Uricase@RBC greatly decreases the uric acid levels in the plasma, thus alleviating hyperuricemia, providing a new alternative for exploring the clinical treatment of hyperuricemia, which is associated with various diseases, such as gout, diabetes, kidney stones, and cardiovascular diseases. Chen and colleagues constructed GOx-Mn nanoparticles (GOx-Mn/HA) by hybridizing a CAT-like Mn-containing nanozyme with GOx to cyclically amplify the consumption of glucose for starvation therapy (Fig. 6B).²¹ Cancer cells use glucose as an energy source to meet fast-growing bioenergetic and biosynthetic

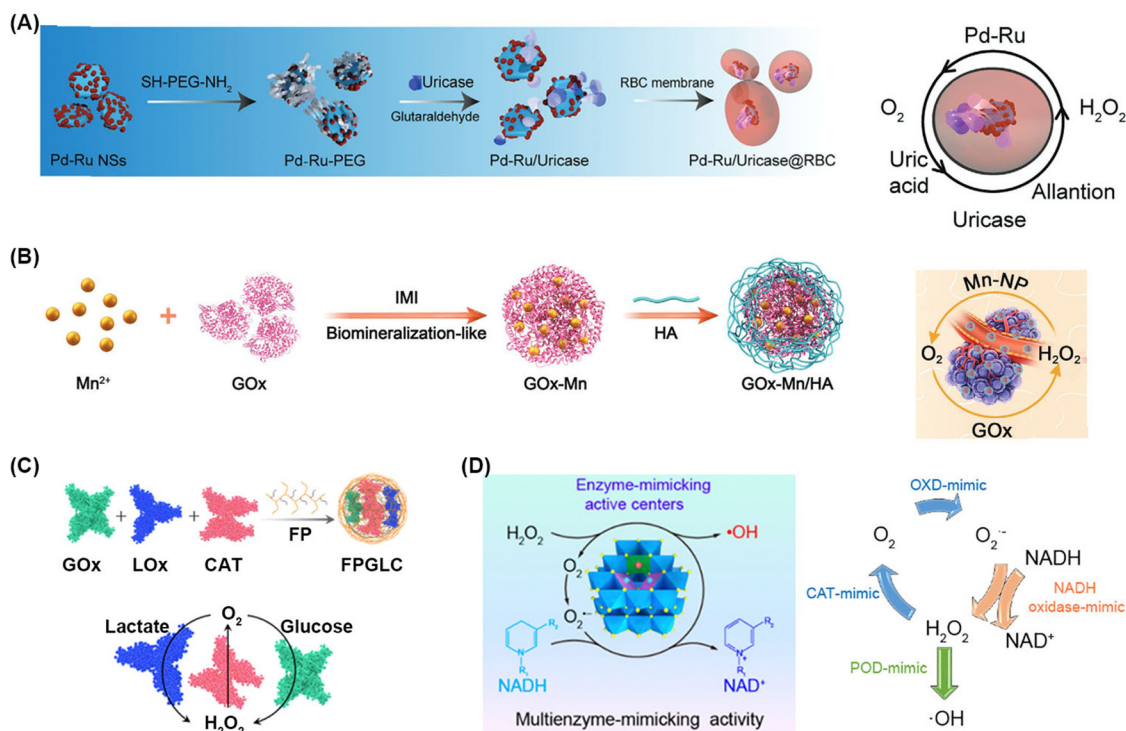


Fig. 6 Representative cyclic cascade reactions induced by enzymes and/or nanozymes. (A) Illustration of the prepared Pd-Ru/uricase@RBC hybrid nanozyme for mediating a cyclic cascade of uricase and CAT. Reprinted (adapted) with permission from ref. 20, copyright 2021, Wiley-VCH. (B) Illustration of the prepared GOx-Mn/HA hybrid nanozyme to cyclically amplify the consumption of glucose using the cyclic cascade reactions induced by GOx-CAT. Reprinted (adapted) with permission from ref. 21, copyright 2022, Wiley-VCH. (C) Procedure for FPGLC synthesis based on fluorinated polymer (FP) co-loaded with GOx, LOx and CAT for the consumption of glucose and lactate in the GOx-CAT and LOx-CAT cyclic cascades, respectively. Reprinted (adapted) with permission from ref. 22, copyright 2022, Wiley-VCH. (D) Schematic illustration of the Fe-MoOv nanozyme mimicking a cyclic cascade of CAT-OXD-NADH oxidase (right). Reprinted (adapted) with permission from ref. 23, copyright 2021, American Chemical Society.

demands. When glucose is consumed, the glucose metabolism for growth is blocked in cancer cells. However, other metabolic pathways in cancer cells can be activated to maintain survival. For example, lactate can compensate for glucose starvation and reduce the efficacy of GOx-mediated starvation therapy because it is a prominent fuel for mitochondrial metabolism. Based on this, Huang and colleagues developed a cascade catalytic system (FPGLC) based on fluorinated polymer (FP) co-loaded with GOx, LOx and CAT (Fig. 6C).²² GOx and LOx consume glucose and lactate, respectively, resulting in abundant H_2O_2 , which is then converted into O_2 by CAT to promote the catalytic reactions of GOx and LOx, leading to the further consumption of glucose and lactate in the GOx–CAT and LOx–CAT cyclic cascades, respectively. Additionally, Lu and colleagues prepared a novel redox nanozyme (Fe–MoOv) that can continuously generate $\bullet\text{OH}$ *via* the cyclic cascade of CAT–OXD–NADH oxidase (Fig. 6D).²³ One consideration of cyclic cascades is that their repetition would lead to the accumulation of the by-product from the first transformation, such as the gluconic acid and pyruvic acid generated from glucose and lactate oxidation, respectively.

2.5 Triangular cascades

In triangular cascades, different catalytic pathways take place simultaneously, starting from the substrate, and then converge to produce the same product. Triangular cascades are the most unconventional biocatalytic cascade reactions. Some have been employed for chemical synthesis, but no triangular cascades have been applied in disease treatment yet.

It is worth noting that the classifications presented above are not strictly applied, as biocatalytic cascade reactions can be classified according to other parameters. The above classifications provide a basic guide to the various cascade catalytic processes. However, biocatalytic cascade design combining different types of cascades may have more advantageous properties and effects. For example, an orthogonal cascade can be combined with a cyclic cascade for H_2O_2 generation, enabling the continuous transformation of H_2O_2 into $\bullet\text{OH}$.¹⁶

3. Biocatalytic cascade reactions in disease management

In modern medicine, chemodrugs still play dominant roles in treating various diseases. However, these drugs inevitably cause severe side effects in patients owing to their poor targeting ability. In addition, chemodrugs lose their therapeutic functionality after interacting with pathogenic/pathological entities, thus high dosage and/or repeated administrations are required, leading to accentuated side effects. With their high catalytic activity and good specificity, enzyme and/or nanozyme-engineered biocatalytic cascade nanoreactors can avoid these issues by using nontoxic enzymes or less toxic nanozymes to react with the intrinsic substrates in pathological regions. Even after disease elimination, the remaining cascade nanoreactors can still play a part in helping to enhance defense mechanisms, facilitating tissue repair and regeneration, and maintaining

homeostasis, with the continuing activities of enzymes or nanozymes, ensuring that the body remains healthy after a disease attack. Notably, continuous enzyme activity requires monitoring, as excessive or unregulated enzymatic activity can potentially cause unwanted side effects or disrupt normal physiological processes. Here, we summarize the studies that have applied enzyme and/or nanozyme-mediated biocatalytic cascade reactions in the management of various diseases, including cancer, oxidative stress-related diseases, wound infections, and hyperuricemia therapy.

3.1 Cancer management

3.1.1 Cancer therapy. As the leading cause of death across the world, cancer has an increasing significant impact on human lives. To treat cancer precisely and effectively, various therapeutic techniques have been developed, such as targeted drug delivery, phototherapy, gene therapy, immunotherapy, and synergistic therapy. However, these therapeutic modalities come with numerous problems owing to their inherent limitations and the complexity of biological environments. With their high degree of effectiveness, good specificity, and reduced side-effects, enzyme and/or nanozyme-triggered biocatalytic cascade reactions are attracting increasing attention for their ability to influence the TME in cancer therapy research. For example, Lin and colleagues employed a single atom Cu nanozyme (Cu SAzyme) with enzymatic activities of CAT, OXD and POD for heat shock protein (HSP)-silencing-induced mild photothermal therapy (PTT) (Fig. 7A).²⁴ Through its CAT-like activity (Fig. 7B), the Cu SAzyme converts the overexpressed H_2O_2 in the TME into O_2 (Fig. 7C), and then activates its OXD-like activity to catalyze the O_2 into $\text{O}_2^{\bullet-}$ (Fig. 7C). Simultaneously, the excess H_2O_2 is also transformed into $\bullet\text{OH}$ through the system's POD-like activity, inducing ROS storm formation (Fig. 7D), which can damage the existing HSPs in cancer cells. When combined with the clinical medicine licogliflozin (LIK066) to close a sodium-dependent glucose transporter valve for blocking the energy required for HSPs synthesis, LIK066-loaded Cu SAzyme exhibits high efficiency in removing HSPs, realizing HSP-silencing induced mild PTT in HeLa human cervical cancer bearing mice (Fig. 7E). Previously, Yang and colleagues developed a defect-engineered nanozyme (AFCT) with multi-enzymatic activities to amplify the efficacy of TME-activated mild PTT (Fig. 7F).²⁵ The AFCT nanozyme, with its SOD-mimicking activity, converts the $\text{O}_2^{\bullet-}$ into H_2O_2 , which is then used to produce highly toxic $\bullet\text{OH}$ through the system's POD-like activity (Fig. 7G), facilitating both apoptosis and ferroptosis in tumor cells. The AFCT nanozyme also exhibits NADH POD-like activity that catalyzes the depletion of NADH in the presence of H_2O_2 . This results in a restricted ATP supply and consequent HSP expression, which alleviates the undesired thermoresistance of tumor cells during the mild PTT process. As such, the AFCT nanozyme achieved synergistic tumor-personalized suppression with a combination of mild PTT, and $\bullet\text{OH}$ -induced apoptosis and ferroptosis in 4T1 breast cancer bearing mice (Fig. 7H and I). Recently, Lin and colleagues incorporated GOx with TME-responsive upconversion

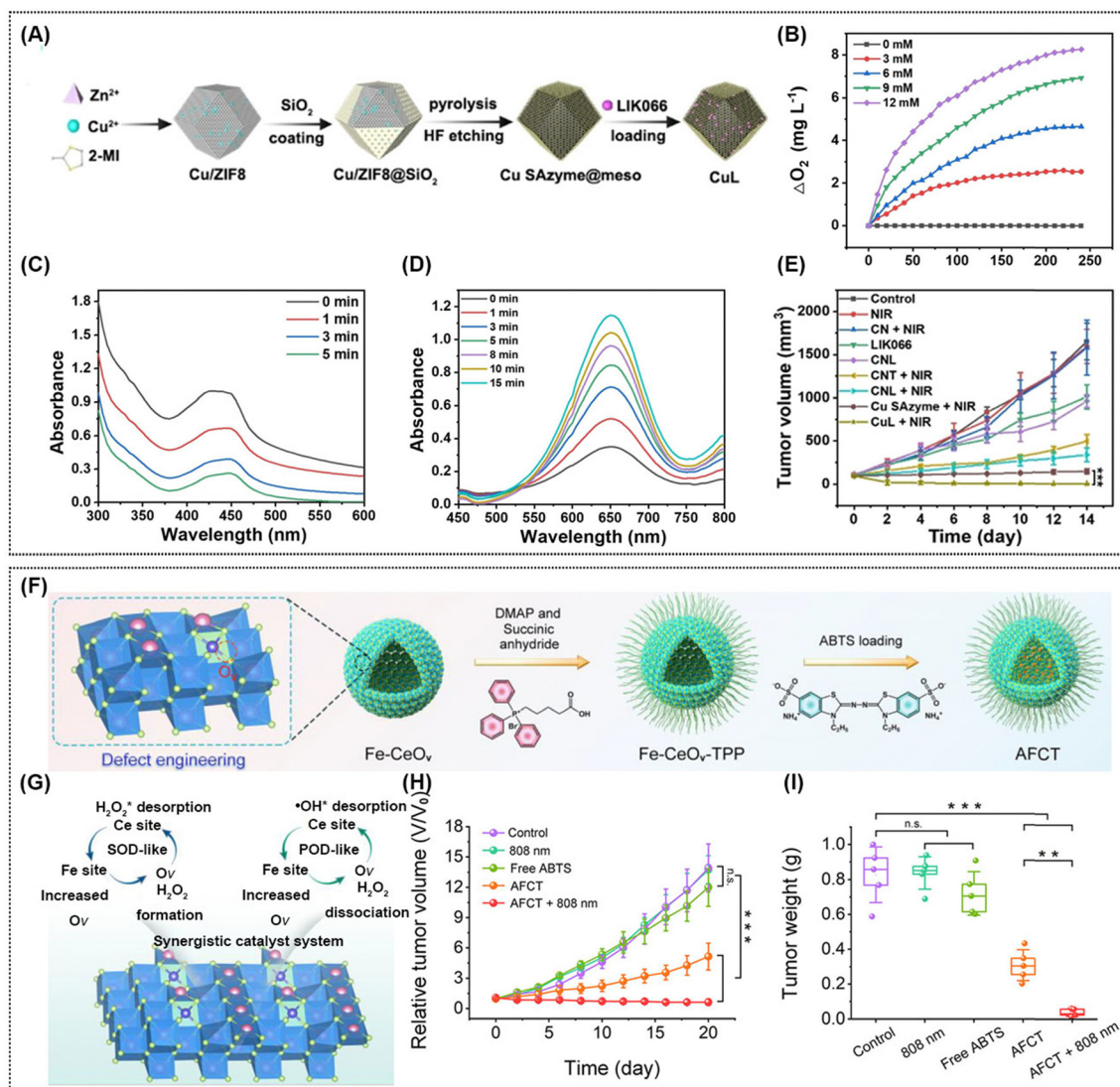


Fig. 7 Representative biocatalytic cascade reactions induced by enzymes and/or nanozymes for cancer therapy. (A) Illustration of the synthetic procedure of Cu SAzyme and CuL. (B) Effect of Cu SAzyme on O₂ generation for CAT-like activity evaluation. (C) Depletion of 1,3-diphenylisobenzofuran due to O₂^{•−} and ¹O₂ generation by OXD-like Cu SAzyme. (D) 3,3',5,5'-Tetramethylbenzidine assay for detecting POD-like activity of Cu SAzyme. (E) Tumor volume in mice after different treatments. **p* < 0.05, ***p* < 0.01, and ****p* < 0.001. Reprinted (adapted) with permission from ref. 24, copyright 2023, Wiley-VCH. (F) Illustration of synthetic processes of AFCT. (G) Schematic representation of the catalysis mechanism of Fe-CeO_x nanozymes. Relative tumor volume (H) and tumor weight (I) of 4T1 tumor-bearing mice with different treatments. ***p* < 0.01, ****p* < 0.001, n.s.: no significance. Data presented as mean ± S.D. (*n* = 5). Reprinted (adapted) with permission from ref. 25, copyright 2023, American Chemical Society.

nanoparticles (UCNPs) to fabricate a UCNPs@Cu-Cys-GOx (UCCG) nanozyme for cancer therapy.²⁶ The prepared UCCG could be specifically activated in the TME to release GOx and Cu²⁺. The released GOx consumes glucose to cut off the nutrient source, thus starving cancer cells accompanied by *in situ* H₂O₂ generation. Meanwhile, Cu²⁺ is reduced to Cu⁺ by GSH *via* a glutathione oxidase (GSHOX)-like activity. Subsequently, Cu⁺ converts H₂O₂ into •OH *via* a POD-like activity, enhancing the CDT effect. In addition, the enhanced •OH generation triggered by GSH depletion not only leads to ferroptosis, but also switches M2 macrophages to the M1 phenotype. When combined with PD-L1 antibody, UCCG showed remarkable antitumor efficacy on bilateral 4T1 tumor-bearing mice. Additionally, this study showed that Cu²⁺ can decrease the expression of glutathione

peroxidase 4 to induce ferroptosis in cancer cells. Considering the important role of ferroptosis in the occurrence and development of various diseases, such as tumors, neurodegenerative diseases, and cardiovascular diseases, Cu²⁺-induced ferroptosis can provide a new strategy for the treatment of these diseases. Although Cu²⁺-mediated ferroptosis has potential applications, it also has certain drawbacks, such as the potential toxicity risks of excessive concentrations of Cu²⁺, lack of specificity in inducing ferroptosis, and limitations of treatment owing to tumor heterogeneity. In addition, further studies are needed to investigate the role and application of Cu²⁺-mediated ferroptosis in non-tumor diseases.

3.1.2 Cancer theranostics. Theranostics, a combination of diagnostics and therapeutics, provides the real-time

identification of tumor location, drug distribution and aggregation, and therapeutic efficacy, and thus is considered a promising strategy for clinical cancer treatment. However, effective theranostic systems remain elusive. With the advances made in nanochemistry and nanocatalysis, enzyme and/or nanozyme-engineered biocatalytic cascade nanoreactors have shown great potential for cancer theranostics. For instance, Huang and colleagues prepared a cyclic cascade catalytic system based on a two-dimensional (2D) PdMo bimetallic nanosheet (PMNS) nanozyme and GOx (PMNSG) for cancer therapy under the navigation of three-dimensional (3D) multi-spectral photoacoustic (PA) imaging (Fig. 8A).²⁷ PMNSG's CAT-like activity catalyzes the conversion of H_2O_2 to O_2 , which is then used by GOx to consume glucose, leading to the generation of abundant H_2O_2 (Fig. 8B). During this cascade catalytic process, the redistribution of O_2 induces the PA signals variation of oxyhemoglobin (OxyHb) and deoxyhemoglobin (DeoxyHb). Combined with the PA response, the authors successfully mapped the 3D PA signals of dynamic OxyHb and DeoxyHb associated with the catalytic process, providing a real-time non-invasive visualization of the tumor (Fig. 8C). Additionally, PMNSG also exhibits POD-like activity that transforms H_2O_2 into $\cdot\text{OH}$, augmenting the efficacy of tumor therapy. An *in vivo* study performed on 4T1 tumor-bearing mice after systemic administration illustrated that PMNSG with laser irradiation was shown to have the greatest inhibition effect on tumor growth, which could also be monitored in real-time with B-mode ultrasonography (Fig. 8D). Additionally, the biocompatible nanoporous TiO_2 hollow spheres with atomic cobalt-dispersed nanozymes (Co/ TiO_2 SAzymes) created by Wang and colleagues not only produce $\text{O}_2\cdot^-$ for killing cancer cells *via* CAT–OXD cascade reactions, but can also load ^{19}F MRI contrast agents or fluorescence dyes to achieve ^{19}F MRI or fluorescence image-guided 4T1 tumor therapy in mice.²⁸ Zhao and colleagues prepared a nanozyme (PHMZCO-AT) by depositing small-molecule 3-amino-1,2,4-triazole (3-AT, an inhibitor of endogenous CAT) into the mesopores or cavities of hollow Mn/Zr-co-doped CeO_2 for imaging the process of intensive CDT (Fig. 8E).²⁹ With its enhanced SOD-like and POD-like activities, PHMZCO-AT nanozyme is capable of converting endogenous $\text{O}_2\cdot^-$ into abundant H_2O_2 , and the elevated H_2O_2 is then used to produce highly toxic $\cdot\text{OH}$ for CDT (Fig. 8F). Simultaneously, the released 3-AT inhibits the activity of endogenous CAT, and thus weakens the off-target decomposition of CAT into H_2O_2 . In addition, the PHMZCO-AT nanozyme also depletes GSH through a redox reaction. As such, the PHMZCO-AT nanozyme achieves intensive CDT. Moreover, owing to the existence of paramagnetic Mn^{2+} and the high X-ray attenuation ability of elemental Zr, PHMZCO-AT can be applied in T_1 -weighted MRI (Fig. 8G) and X-ray computed tomography imaging (Fig. 8H) of the therapeutic process in 4T1 tumor-bearing mice. Additionally, the $\text{Fe}_3\text{O}_4/\text{Ag}/\text{Bi}_2\text{MoO}_6$ nanozyme not only employs the SOD–CAT cascade to replenish H_2O_2 , allowing the POD–GSHOD cascade to sustainably produce $\cdot\text{OH}$ for killing cancer cells, but also shows strong NIR-II absorption properties due to the doping of Fe_3O_4 and Ag NPs. Thus, this nanozyme facilitates advanced MRI, PA, and photothermal image-guided nanocatalytic therapies in 4T1 tumor-bearing mice.¹⁶

Generally, solid tumors are characterized by a hypoxic environment that can have multiple effects on the activity of biocatalytic cascades. First, hypoxia may inhibit the activity of biocatalytic cascades. For example, GOx can efficiently catalyze glucose under aerobic conditions, however, its catalytic efficiency is significantly inhibited in hypoxic environments. Second, hypoxia can alter the metabolism of tumor cells, affecting the supply of substrates required for enzyme-catalyzed reactions. For example, the ratio of NAD^+ to NADH differs under aerobic and anaerobic conditions, which may affect the activities of enzymes that rely on these cofactors. Third, hypoxia may affect the stability and further conversion of intermediates because intermediates may be rapidly converted into subsequent substances under aerobic conditions, however, under hypoxic conditions, these intermediates may accumulate or undergo different chemical reactions. To achieve efficient tumor therapy and theranostics, it is necessary to optimize the enzymes or nanozymes of the biocatalytic cascades.

3.2 Oxidative-stress-associated disease management

Oxidative stress is associated with many acute and chronic inflammatory diseases, yet only a limited number of treatments are currently available for clinical use. As diverse antioxidant enzymes, such as SOD, CAT, and GPx, play vital roles in maintaining intracellular redox homeostasis, thus multiple anti-oxidases or antioxidant-mimicking nanozymes have been used to construct cascade nanoreactors for the management of oxidative-stress-associated diseases. Examples of these applications are provided below.

3.2.1 Neurodegenerative disease therapy. Traumatic brain injury (TBI) is a major degenerative brain disease associated with posttraumatic stress disorder, memory deficits, and chronic neuroinflammation. According to the pathophysiological process of TBI, it can be divided roughly into two forms: primary injury and secondary injury. Secondary injury occurs after primary injury and triggers continuous changes in neuronal physiological activity and metabolism, leading to long-lasting secondary neuronal and glial damage, including neuroinflammation, brain edema, and nerve cell death. To mitigate secondary brain damage after TBI, the inhibition of oxidative stress is essential, as TBI-induced oxidative stress plays a pivotal role in its pathological progression. As such, Zhang and colleagues developed an oligomeric nanozyme O-NZ with comparable natural activities of SOD and GPx to alleviate TBI-induced oxidative stress.¹⁰ With its SOD-like activity, the O-NZ nanozyme converts $\text{O}_2\cdot^-$ into O_2 and H_2O_2 , and the produced H_2O_2 is decomposed into H_2O *via* the nanoenzyme's GPx-like activity. The O-NZ nanozyme also exhibits excellent $\cdot\text{OH}$, $\text{NO}\cdot$, and ONOO^- scavenging activities. Accordingly, the O-NZ nanozyme was found to significantly relieve oxidative stress and thus increase the overall survival rate of mice with severe TBIs from 50% to 90%, and greatly promote the recovery of their long-term neurocognition. Xue and colleagues synthesized Janus catalysis-driven nanomotors (JCNs) with multienzyme-like catalytic activities for the emergency rescue of TBI (Fig. 9A).³⁰ When the JCNs were dropped onto the surface of a ruptured

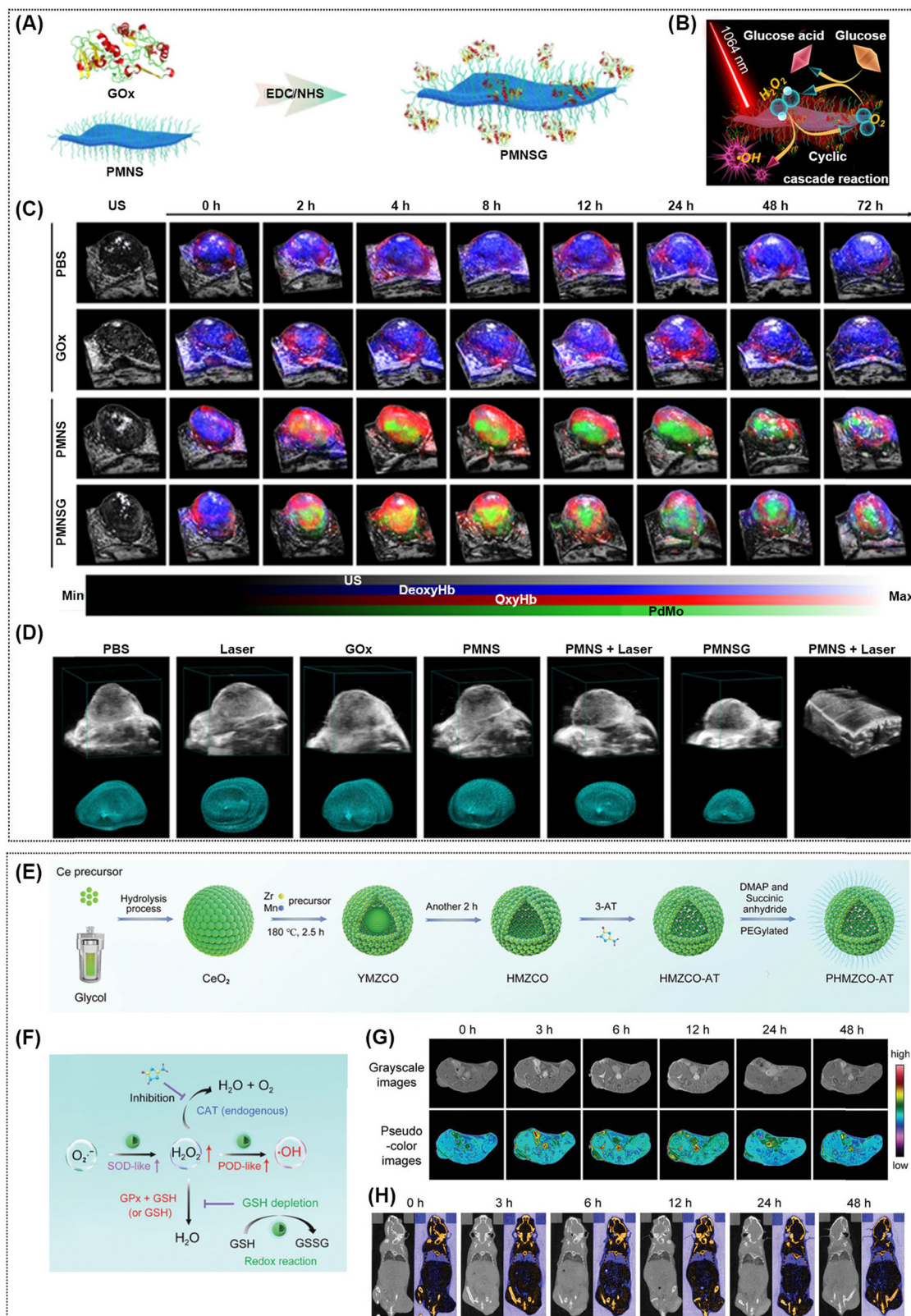


Fig. 8 Representative biocatalytic cascade reactions induced by enzymes and/or nanozymes for cancer theranostics. (A) Illustration of the preparation of PMNSG. (B) The photothermal enhanced cyclic cascade reaction of PMNSG under 1064-nm laser irradiation. (C) PA imaging monitoring of OxyHb, DeoxyHb and PdMo on 4T1 tumor-bearing mice in real-time after systemic administration of different treatments. (D) B-Mode US images of a 4T1 tumor with the 3D reconstruction of the tumor region with different treatments. Reprinted (adapted) with permission from ref. 27, copyright 2022, Springer Nature. (E) Illustration of the synthetic procedure of PHMZCO-AT nanozymes. (F) Illustration of the cascade catalytic process of PHMZCO-AT nanozymes in cells. T_1 -Weighted MR imaging (G) and X-ray computed tomography imaging (H) of 4T1 tumor-bearing BALB/c mice intravenously injected with PHMZCO-AT nanozymes at various time points. Reprinted (adapted) with permission from ref. 29, copyright 2022, Wiley-VCH.

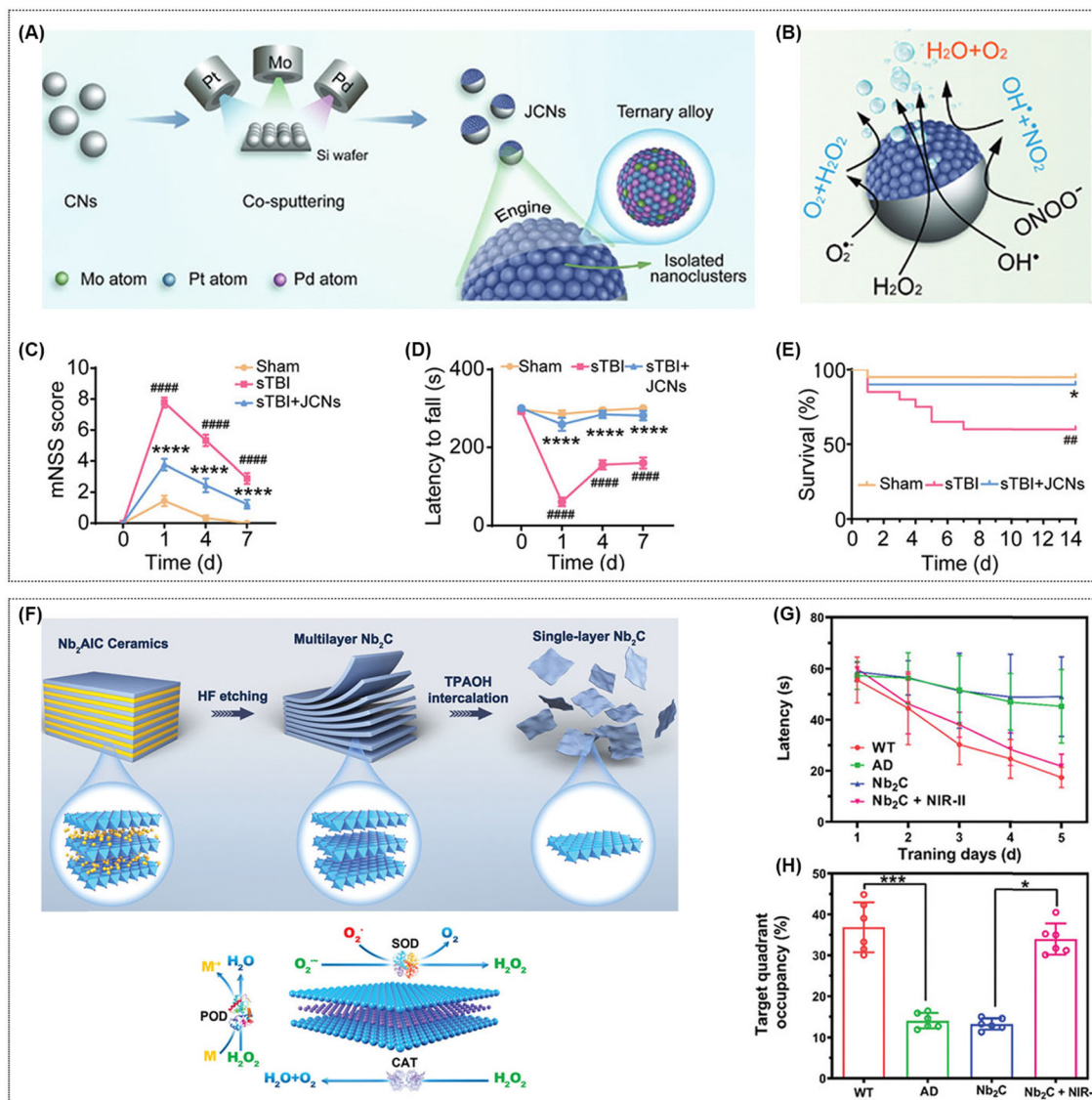


Fig. 9 Representative biocatalytic cascade reactions induced by enzymes and/or nanozymes for neurodegenerative disease therapy. (A) Preparation of self-propelled Janus catalysis-driven nanomotors (JCNs). (B) Illustration of cascade catalysis induced by JCNs. (C) Modified neurological severity score (mNSS) test with or without JCNs treatment at various time points post injury. (D) Recovery of motor function by rotor-rod analysis at different time points post injury after different treatments. (E) Survival rate during 14 days with different treatments. Data are expressed as mean \pm S.E.M. ($n = 9$, $^{\#}p < 0.01$, $^{\#\#}p < 0.001$, $^{\#\#\#}p < 0.0001$ vs. Sham group; $^*p < 0.05$, $^{**}p < 0.01$, $^{***}p < 0.001$, $^{****}p < 0.0001$ vs. sTBI group). Reprinted (adapted) with permission from ref. 30, copyright 2022, Wiley-VCH. (F) Illustration of the delamination and disintegration of ultrathin Nb_2C nanosheets and its cascade catalytic process. (G) Escape latency of mice with different treatments ($n = 6$). (H) Percentage of target quadrant occupancy on the probe trial day after different treatments ($n = 6$, $^*p < 0.05$, $^{**}p < 0.01$, and $^{***}p < 0.001$). Reprinted (adapted) with permission from ref. 31, copyright 2022, Wiley-VCH.

skull, they effectively catalyzed the decomposition of endogenous H_2O_2 to generate O_2 bubbles, which served as the fuel to promote the movement of the JCNs to deep brain lesions, where they activated SOD-CAT cascade reactions to scavenge $\text{O}_2^{\bullet-}$, as well as $\bullet\text{OH}$, and ONOO^- (Fig. 9B), thus dramatically reversing the severe oxidative stress and subsequent inflammatory cascade response at lesion sites. The JCNs were found to successfully recover behavioral defects and cognitive impairments in TBI mice (Fig. 9C–E).

Alzheimer's disease (AD) is a neurodegenerative disease characterized by progressive cognitive deterioration and memory attrition. Though pathogenesis of AD has not been fully

established, several abnormal changes, such as acetylcholine deficits, amyloid- β ($\text{A}\beta$) oligomer aggregations, neuroinflammation, elevated oxidative stress, and the dyshomeostasis of biometals have been proven to play important roles in AD progression. Accordingly, biocatalytic cascade reactions aiming to relieve oxidative stress have been designed as potential AD therapies. For example, Qu and colleagues developed a biocompatible cascade nanoreactor, NSC@PCN/HOF, for use in ameliorating the pathological symptoms related to AD.⁸ With its PCN nanozyme activity, NSC@PCN/HOF can efficiently remove $\text{O}_2^{\bullet-}$ by a SOD-CAT cascade reaction, thus protecting NSCs from oxidative stress. NSC@PCN/HOF was shown to

prevent the loss of NSC stemness and reduce the cytomembrane damage caused by syringe needle injection during NSC transplantation, achieving enhanced NSC viability, promoting neurogenesis, and relieving cognitive disorders in aged $3 \times \text{Tg-AD}$ mice. Notably, increasing evidence suggests that excessive Cu^{2+} catalyzes the formation of ROS, which cause oxidative damage and neurotoxicity. Therefore, Zhang and colleagues developed a cascade nanocatalyst based on a 2D Nb_2C MXene nanosheet for binding toxic Cu^{2+} and scavenging excessively generated ROS (Fig. 9F).³¹ The Nb_2C MXene selectively captures Cu^{2+} to suppress the interaction between Cu^{2+} and $\text{A}\beta$ aggregates, protecting neuronal cells from Cu^{2+} -associated toxicity. Additionally, its SOD- and CAT-like activities can promote a SOD–CAT cascade to scavenge $\text{O}_2^{\bullet-}$. The Nb_2C MXene also exhibits H_2O_2 - and $\bullet\text{OH}$ -scavenging abilities, and thus can greatly alleviate oxidative damage. With their selective Cu^{2+} -chelating and ROS-scavenging properties, the 2D Nb_2C nanosheets were able to efficiently inhibit neuroinflammatory responses and showed neuroprotective effects in an $\text{A}\beta$ precursor protein/presenilin-1 double-transgenic AD mouse model (Fig. 9G and H).

Li and colleagues developed a biocatalytic cascade nanosystem based on a 2D vanadium carbide (V_2C) MXene for treating Parkinson's disease (PD).³² Under physiological conditions, the V_2C MXene can mimic up to six naturally-occurring enzymes, including SOD, CAT, POD, GPx, thiol peroxidase (TPx) and haloperoxidase (HPO). Thus, the nanosystem not only effectively converts $\text{O}_2^{\bullet-}$ into O_2 and H_2O through the linear cascades of SOD–POD and SOD–CAT, but also eliminates H_2O_2 and $\bullet\text{OH}$ by employing GPx-, TPx-, and HPO-like catalytic activities. These activities were demonstrated to significantly ameliorate neuroinflammation in PD mice by inhibiting oxidative stress.

3.2.2 Ischemia-reperfusion injury therapy. Ischemia-reperfusion injury (IRI) occurs when there is a cessation and

restoration of blood supply during surgeries, such as arterial bypass grafting, thrombolytic therapy, cardiopulmonary bypass cardiac surgery, cardiopulmonary cerebral resuscitation, and organ transplantation. IRI may result in an acute inflammatory response, severe organ damage, and even organ failure and death. The mechanisms of IRI have not been fully elucidated, but a well-characterized initiating factor is a burst of $\text{O}_2^{\bullet-}$ from the mitochondrial respiratory chain upon reperfusion. Thus, protecting mitochondria from $\text{O}_2^{\bullet-}$ -induced damage is essential in alleviating IRI. Based on this, Chen and colleagues integrated ultrasmall platinum nanoparticles (Pt NPs) and natural nitric oxide synthase (iNOS) into the zeolitic imidazolate framework-8 (ZIF-8) to form a cascade nanoreactor (Pt–iNOS@ZIF) that can be used in the prevention of hepatic IRI.⁹ Due to their SOD-like activity, the Pt NPs efficiently transform $\text{O}_2^{\bullet-}$ into O_2 and H_2O_2 . The generated H_2O_2 is then converted into H_2O and O_2 via CAT-like activity, and the generated O_2 can be used by iNOS to produce NO in the presence of L-arginine. With ROS clearance and NO generation, Pt–iNOS@ZIF greatly reduce oxidative stress and the expression of proinflammatory cytokines, potentially leading to an effective intervention for hepatic IRI in a murine model. Recently, Liu and colleagues constructed a cascade antioxidant system based on an $\text{Fe}_2\text{NC}@ \text{Se}$ nanozyme by encapsulating a dual-Fe-atom nanozyme (Fe_2NC) within a selenium-containing metal–organic framework (Se-MOF) shell layer as an agent for ameliorating cerebral IRI (Fig. 10A).³³ As with Pt–iNOS@ZIF, the prepared Fe_2NC nanozyme exhibits high SOD-like and CAT-like catalytic activities, and thus efficiently removes $\text{O}_2^{\bullet-}$ via SOD–CAT cascade catalytic reactions. The excessive H_2O_2 is also reduced to H_2O by the GPx-like Se-MOF under physiological conditions. In an *in vivo* demonstration, the $\text{Fe}_2\text{NC}@ \text{Se}$ nanozyme was able to markedly protect middle cerebral artery occlusion (MCAO) mode rats from injury by decreasing the infarct volume and

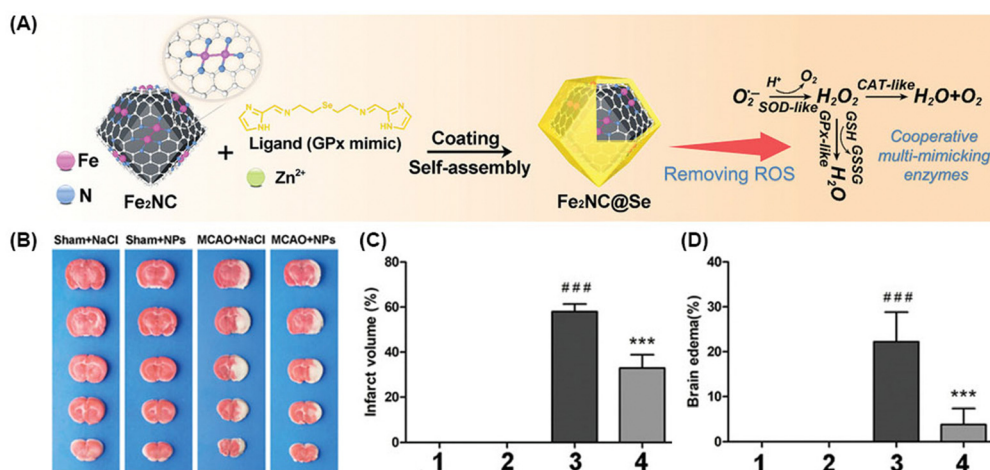


Fig. 10 $\text{Fe}_2\text{NC}@ \text{Se}$ nanozyme with multi-enzyme cascade activities to protect against cerebral IRI. (A) Illustration of the prepared $\text{Fe}_2\text{NC}@ \text{Se}$ nanozyme to remove ROS through cascade catalytic reactions. (B) Representative of 2,3,5-triphenyl tetrazolium chloride staining images of brain slices of Sham + NaCl (1), Sham + NPs (2), MCAO + NaCl (3) and MCAO + NPs (4) groups. Infarct volume (C) and brain edema (D) after different treatments ($n = 5$). All data were expressed as mean \pm SD. # # denotes $p < 0.01$ compared with Sham + NaCl group, # # # denotes $p < 0.001$ compared with Sham + NaCl group, *** denotes $p < 0.001$ compared with MCAO + NaCl group. Reprinted (adapted) with permission from ref. 33, copyright 2022, Wiley-VCH.

improving neurological deficits (Fig. 10B–D). Huang and colleagues developed a mitochondria-target cascade nanozyme (Mito-fenzyme) for use in the targeted treatment of cardiac IRI.³⁴ The hybrid nanozyme is capable of the cascade conversion of $O_2^{\bullet-}$ into nontoxic O_2 and H_2O via its SOD- and CAT-like activities, while generating negligible amounts of $\bullet OH$ generation owing to its lower POD-like activity. Mito-fenzyme was shown to alleviate mitochondrial oxidative injury and improve the functional recovery of cardiac tissues in mouse models after cardiac IRI. More recently, Fan and colleagues reported their development of a thrombin-activated nanozyme-based cascade catalytic system, using self-assembling polypeptides to generate a peptide-templated manganese dioxide nanozyme (PNzyme/ MnO_2) for treating reperfusion injury in ischemic stroke (IS).³⁵ Through a multilevel targeting strategy, the PNzyme/ MnO_2 nanozyme first targets the thrombi to initiate thrombolytic activity, and subsequent secondary and tertiary targeting to guide further positioning ischemic tissue, where it disposes of the $O_2^{\bullet-}$ produced after thrombolysis and reperfusion through SOD–CAT cascade reactions, alleviating oxidative injury in mitochondria and enhancing neurological functional recovery in mice and rat IS models. As such, PNzyme/ MnO_2 has the potential to improve therapeutic efficacy and prevent secondary thrombosis during the treatment of IS.

3.2.3 Kidney disease therapy. Acute kidney injury (AKI) is a severe renal dysfunction syndrome associated with the excess production of ROS and reactive nitrogen species (RNS). Although the U.S. Food and Drug Administration has approved the use of amifostine's free-radical scavenging ability to alleviate AKI, its side-effects and low efficacy limit its clinical utilization. Recently, cascade catalytic nanoreactors constructed with multiple enzymes or their mimics have arisen as alternative therapies for AKI. For example, Peng and colleagues rationally designed $KCa(H_2O)_2[Fe^{III}(CN)_6] \cdot H_2O$ nanoparticles (CaPB NPs) as multienzyme mimetics for use in treating AKI (Fig. 11A and B).³⁶ The CaPB NPs mimic the activities of multiple enzymes, including SOD (Fig. 11C), CAT (Fig. 11D), POD (Fig. 11E), and GPx (Fig. 11F). CaPB NPs employ their SOD-like activity to transform $O_2^{\bullet-}$ into O_2 and H_2O_2 , and subsequently activated CAT-, POD-, and GPx-like activities convert the excessive H_2O_2 into O_2 and/or H_2O . CaPB NPs could also effectively scavenge $\bullet OH$ and RNS to protect the kidney from oxidative injury (Fig. 11G and H). In addition, the CaPB NPs serve as a robust ferroptosis inhibitor to increase the expression of glutathione peroxidase 4. With their highly effective ROS/RNS-scavenging abilities and targeted inhibition of ferroptosis, the CaPB NPs exhibited effective therapeutic performance in an IR-induced AKI mouse model.

Oxidative stress is a prominent pathogenic mechanism in the early stages of chronic kidney disease (CKD), a condition characterized by the progressive and permanent loss of renal functions. Currently, only kidney replacement and blood purification interventions are clinically available for the treatment of CKD. However, most CKD patients undergoing blood purification exhibit added oxidative stress due to the poor biocompatibility of the devices, multiple complications, as well as the

hemodialysis procedure itself. Additionally, current antioxidants show poor activities and potential side effects. Therefore, Zhao and colleagues formulated a series of antioxidative cascade metal–phenolic nanozymes (M–TA NMs) with active sites that can be regulated by varying their content of metal (Cu^{2+} , Zn^{2+} , Na^+ , and K^+) or nonmetal (NH_4^+) ions (Fig. 11I).³⁷ Among these M–TA NMs, Cu–TA NMs showed the best SOD- and CAT-like catalytic activities, efficiently converting $O_2^{\bullet-}$ into O_2 and H_2O_2 , the latter of which is further transformed into O_2 and H_2O . Cu–TA NMs can also act as efficient $\bullet OH$ and RNS scavengers. In extracorporeal hemoperfusion, Cu–TA₂-engineered polymeric microspheres (Cu–TA₂@PMS) effectively eliminate ROS in the complex blood environment, demonstrating the potential for oxidative stress alleviation during blood purification and preventing the progression of CKD (Fig. 11J).

3.2.4 Acute liver injury therapy. Acute liver injury (ALI) is a serious disease with high mortality, characterized by the rapid loss of hepatocyte functions in previously healthy individuals. Excessive ROS generation has been identified as a vital pathological hallmark closely related to the occurrence and progression of ALI. Based on this, Deng and colleagues reported their design of a cascade nanocatalytic system containing ultrasmall $Cu_{5.4}O$ NPs for the treatment of ALI.³⁸ The $Cu_{5.4}O$ USNPs catalyze $O_2^{\bullet-}$ transformation into H_2O_2 through their SOD-like activity, and the produced H_2O_2 is then decomposed by CAT-like activity into H_2O and O_2 , or by GPx-like activity into H_2O . Simultaneously, the $Cu_{5.4}O$ USNPs can also efficiently scavenge $\bullet OH$. With the benefits of their robust ROS scavenging ability, the $Cu_{5.4}O$ USNPs exhibited outstanding therapeutic effects in an ALI mouse model, as well as AKI and diabetic wound models.

3.2.5 Inflammatory bowel disease therapy. Inflammatory bowel disease (IBD), also referred to as “green cancer”, is a common chronic gastrointestinal inflammatory disease. Current treatments mainly include the oral administration of 5-aminosalicylic acid and other anti-inflammatory drugs that relieve the symptoms of IBD. However, these drugs exhibit limited therapeutic effects, and serious toxic side effects, such as the increased risk of infections and malignant tumors. Inspired by cellular anti-ROS pathways that use ROS-scavenging enzymes, Liu and colleagues developed an integrated mimetic cascade nanozyme (Pt@PCN222-Mn) able to scavenge ROS to treat IBDs, including Crohn's disease (CD) and ulcerative colitis (UC).³⁹ The SOD-like activity of Pt@PCN222-Mn converts $O_2^{\bullet-}$ into O_2 and H_2O_2 , the latter of which is further catalyzed into H_2O and O_2 by CAT-like activity. In mouse studies, Pt@PCN222-Mn exhibited superior therapeutic efficacy in both UC and CD model states. In addition, Wei and colleagues developed a self-cascading nanozyme $LiMn_2O_4$ (LM) with multiple antioxidant enzymes with SOD-, GPx-, and CAT-like activities for IBD therapy.⁴⁰ By employing SOD–CAT cascade reactions, the LM efficiently catalyzes the conversion of $O_2^{\bullet-}$ into H_2O and O_2 . The GPx-mimicking LM then synergistically decomposes H_2O_2 into innocuous products, providing a cascade antioxidant system that was used to successfully treat IBD in mice.

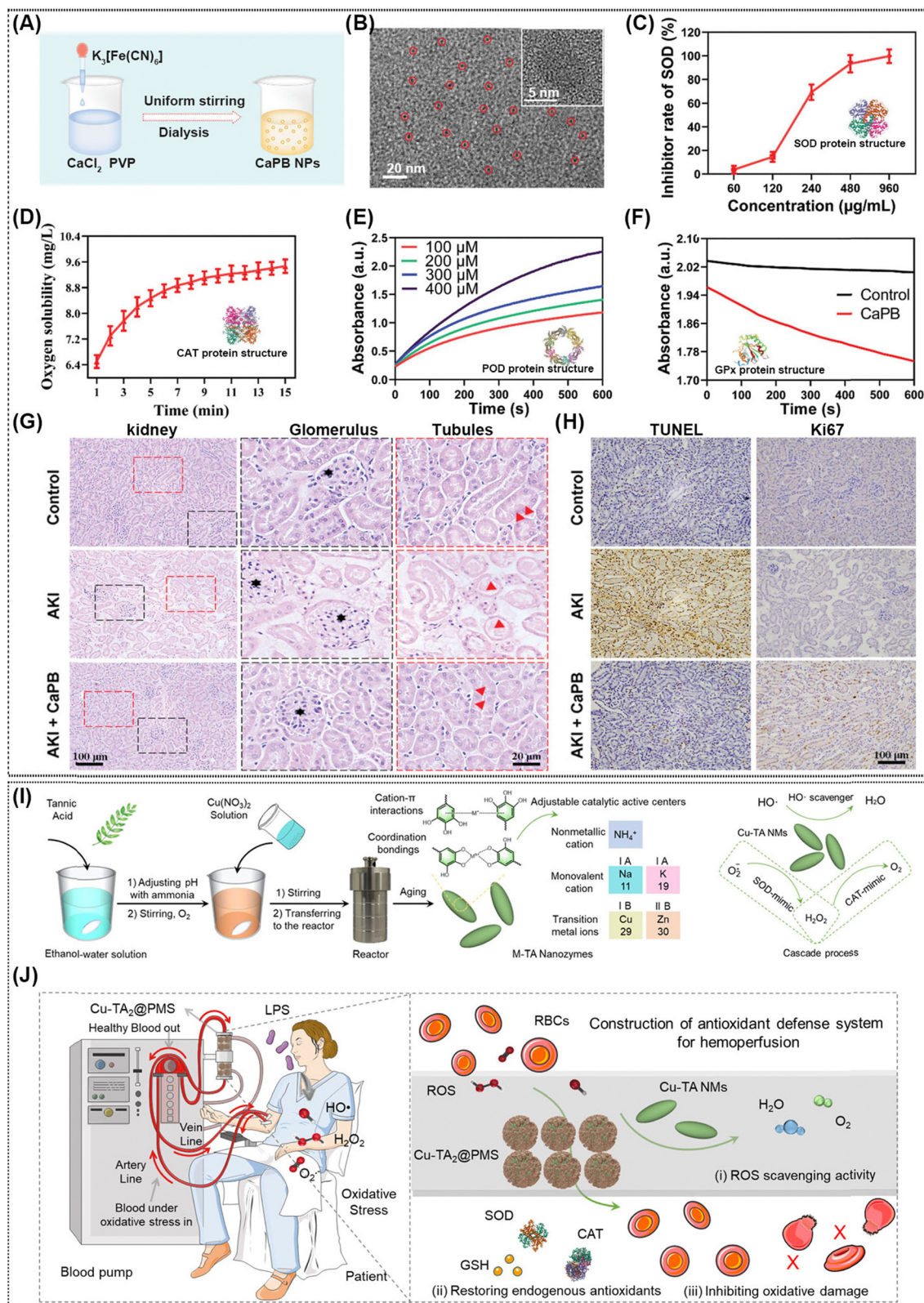


Fig. 11 Representative biocatalytic cascade reactions induced by enzymes and/or nanozymes for kidney disease therapy. (A) Schematic preparation of CaPB NPs. (B) Transmission electron microscope image of CaPB NPs. Evaluation of SOD-like activity (C), CAT-like activity (D), POD-like activity (E), and GPx-like activity (F) of CaPB NPs. (G) Hematoxylin and eosin staining of kidneys with different treatments. Kidney tissues with the glomerulus represented by the black pentagram and the brush borders in tubules represented by the red triangle. (H) Terminal deoxynucleotidyl transferase-mediated dUTP nick end labeling (TUNEL) assay (brown nuclei) and immunohistochemical staining with Ki67 (brown) in AKI mice after different treatments. Reprinted (adapted) with permission from ref. 36, copyright 2022, Wiley-VCH. (I) Illustration of the synthesis of M-TA NMs and its ROS-scavenging capacities. (J) Illustration of dynamic hemoperfusion and protective mechanisms for oxidative stress of Cu-TA₂@PMS. Reprinted (adapted) with permission from ref. 37, copyright 2022, American Chemical Society.

Oral probiotic therapeutics are promising adjuvants that could be used to treat IBD by modulating the gut bacterial composition and promoting intestinal mucosal repair. An artificial-enzyme-armed *Bifidobacterium longum* probiotic (BL@B-SA₅₀) has been formulated for IBD treatment (Fig. 12A).⁴¹ The BL probiotic promotes the targeting and retention of BL@B-SA₅₀, allowing it to persistently scavenge O₂^{•−} and [•]OH through SOD-CAT cascade and redox reactions, respectively, and thus alleviate inflammatory factors. Because of the reduced inflammation, the probiotics are protected from oxidative damage and can rapidly reshape intestinal barrier function and restore the gut microbiota. As such, the BL@B-SA₅₀ exhibited prominent therapeutic potential in murine models of UC and CD and beagle dogs challenged with colitis (Fig. 12B and C).

3.2.6 Arthritis therapy. Arthritis is a chronic inflammatory disease of the joints, the most common causes of which are osteoarthritis (OA) and rheumatoid arthritis (RA). OA, also known as degenerative joint disease, is characterized by synovial inflammation, progressive cartilage loss, and osteophyte formation. Surgery and pharmacological treatments are the most common conventional therapeutic strategies for OA, but they often fail to achieve the desired outcomes. Studies have revealed that the overproduction of ROS in the arthrosis microenvironment leads to the progression and is part of the pathogenesis of OA. As such, Zhao and colleagues developed a graphene-supported Cl-Cu-N₄-centered SAzyme (Cu-N₄ClG)

with SOD- and CAT-like catalysis activities to treat OA.⁴² Owing to its high SOD-like activity, Cu-N₄ClG SAzyme can efficiently transform O₂^{•−} into H₂O₂ and O₂, sequentially implementing its CAT-like activity to decompose the excessive H₂O₂ into H₂O and O₂. Cu-N₄ClG SAzyme is also endowed with an RNS-scavenging ability, by which it can synergistically protect chondrocytes from oxidative stress-induced apoptosis and alleviate OA in Sprague-Dawley rats.

RA is a widespread and devastating systemic autoimmune disease that affects synovial joints. Traditional anti-rheumatic therapeutics, such as glucocorticoids, antirheumatic drugs, and nonsteroidal anti-inflammatory drugs, can rapidly relieve RA symptoms in the early stages. However, their further application is limited due to drug resistance, poor bioavailability, and adverse effects. Despite the progress that has been made in developing biological antirheumatic drugs to suppress proinflammatory cytokines, such as tumor necrosis factor- α and interleukin 6, RA patients have failed to respond better to these than conventional antirheumatic drugs. More recently, specific determinants in the RA microenvironment, such as hypoxia and ROS, have been considered as potential targets for therapies aiming to stem the uncontrolled progression of RA. Shi and colleagues constructed a composite nanomedicine (MHPH) that can deplete intracellular ROS for the treatment of RA.⁴³ MHPH responds to the mild acidic environment to concurrently release Mn²⁺ and H₂TE-2-PyP⁴⁺, which enables

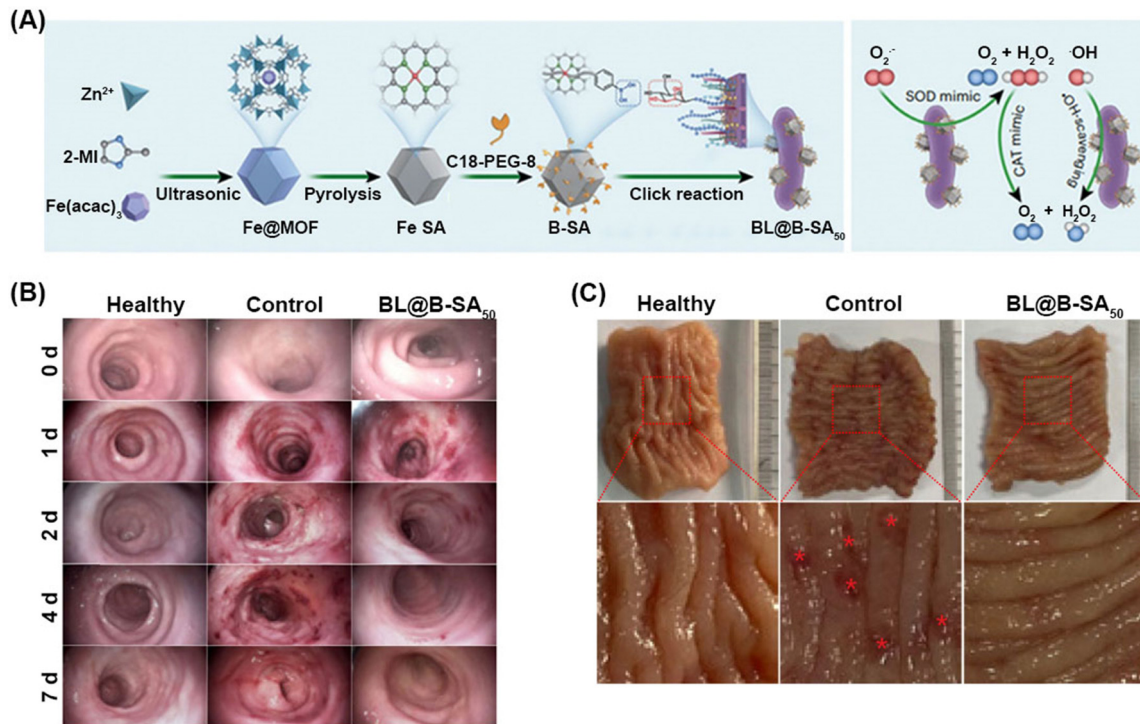


Fig. 12 Artificial-enzyme-modified *Bifidobacterium longum* probiotics (BL@B-SA₅₀) for reshaping a healthy immune system in IBD. (A) Illustration of the preparation of BL@B-SA₅₀ for scavenging multiple ROS. (B) Representative endoscopic photographs of dogs with different treatments at different time points. (C) Representative photographs of colons obtained from dogs after different treatments at day 7. Healthy group: healthy dogs given medium; control group: UC dogs given medium; BL@B-SA₅₀ group: UC dogs orally administered with BL@B-SA₅₀. Reprinted (adapted) with permission from ref. 41, copyright 2023, Springer Nature.

the synthesis of MnTE-2-PyP⁵⁺ with the catalytic activities of Mn-SOD and CAT (Fig. 13A). Using its Mn-SOD-like activity, MnTE-2-PyP⁵⁺ efficiently converts intracellular O₂^{•−} into O₂ and H₂O₂, and the generated H₂O₂ is subsequently decomposed into O₂ and H₂O *via* its CAT-like activity. This reduces ROS levels in M1 macrophages and facilitates a shift from the M1 to the M2 phenotype. Additionally, the Si-containing oligomers released from the MHPH promote biomineralization and bone regeneration (Fig. 13B and C). In an RA mouse model, the authors found that a single administration of MHPH exhibited higher antiarthritic efficacy than the typically used antioxidant ascorbic acid, which must be administered multiple times.

Diabetic osteoporosis is associated with systemic glucose metabolism-disorder-induced bone microstructure damage, reduced bone strength, fracture susceptibility, and bone defects in diabetes mellitus patients. It has been reported that the overproduction of ROS and high glucose levels confer a

negative effect on bone regeneration. Therefore, reducing glucose and ROS in diabetic bone defects should be beneficial for bone regeneration. To address this, Huang and colleagues designed a 3D-printed enzyme-functionalized scaffold (Alg/GOx/CaP@CAT) for the cascade catalytic therapy of diabetic bone defects (Fig. 14A).⁴⁴ After implantation, the Alg/GOx/CaP@CAT not only efficiently catalyzes glucose into gluconic acid and H₂O₂ (Fig. 14B), the latter of which is then decomposed by CAT into H₂O and O₂ (Fig. 14C), but also scavenges the excess H₂O₂, thus reducing glucose and ROS levels. In addition, Alg/GOx/CaP@CAT facilitates bone regeneration *via* the production of Ca²⁺ and PO₄^{3−} (Fig. 14D and E). The evidence reveals that the 3D-printed enzyme-functionalized scaffold could provide an effective strategy for diabetic bone tissue regeneration in a type 2 diabetic rat model.

3.2.7 Atherosclerosis therapy. Atherosclerosis (AS) is a chronic progressive disease characterized by lipid deposition

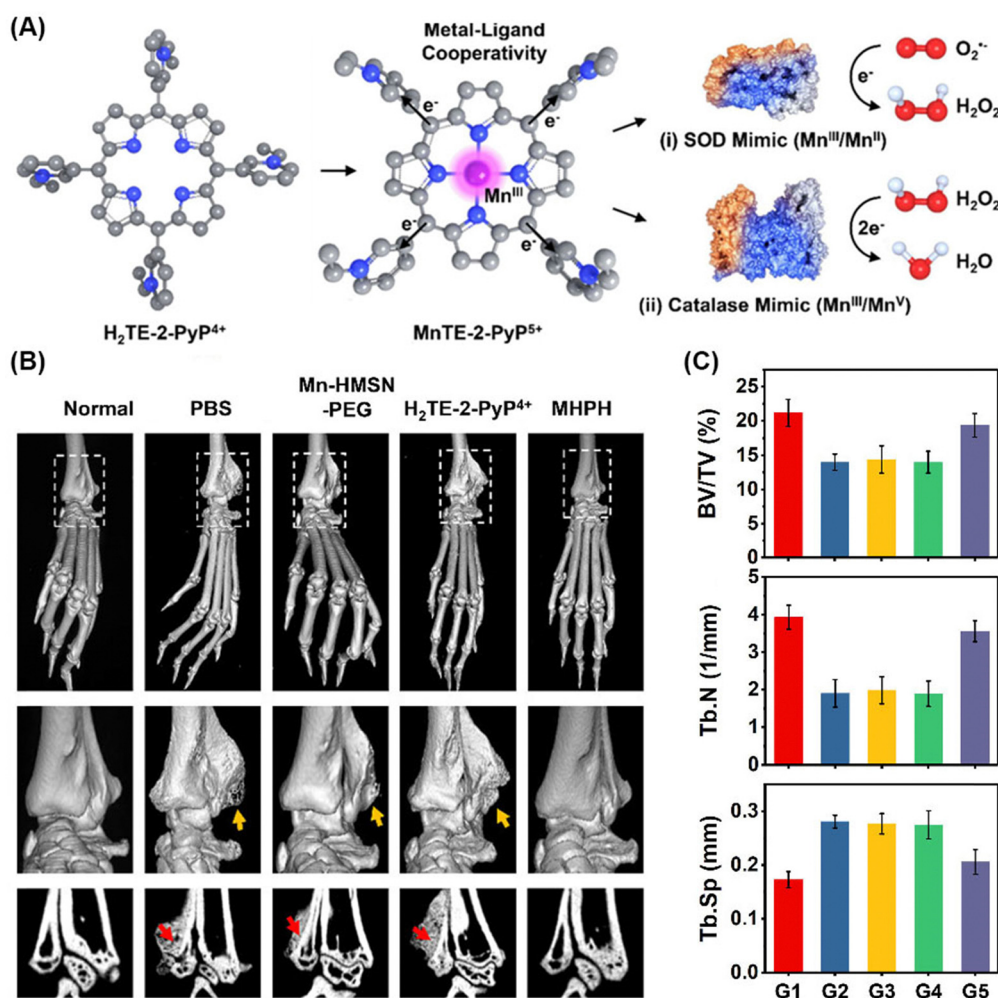


Fig. 13 (A) Illustration of MHPH nanomedicine for *in situ* synthesis of manganese porphyrin bearing SOD and catalase-like activities. (B) 3D-Reconstructed micro-CT images of right hind ankle joints of normal and arthritic mice after different treatments on day 36, with low and high magnifications, as well as original micro-CT images for trabecular. The yellow and red arrows indicate bone erosion. (C) Histomorphometric analysis of bone microstructure for right hind ankle joints of normal and arthritic mice after different treatments on day 36. BV/TV: bone volume/total volume, Tb.N: trabecular number, Tb.Sp: trabecular separation. G1–G5: normal group, PBS group, Mn-HMSN-PEG group, H₂TE-2-PyP⁴⁺ group, MHPH group. Data are expressed as means \pm SD ($n = 5$). Reprinted (adapted) with permission from ref. 43, copyright 2022, American Chemical Society.

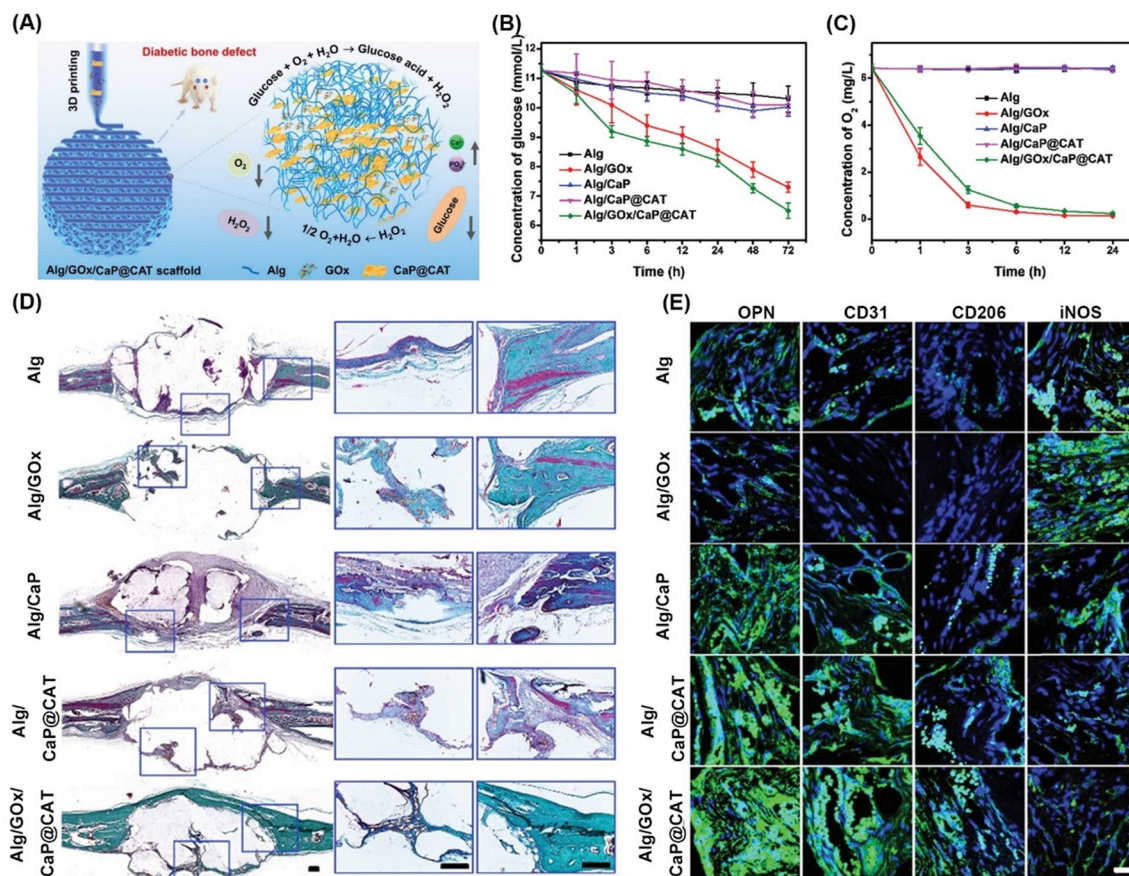


Fig. 14 (A) Illustration of 3D printed Alg/GOx/CaP@CAT scaffolds and its cascade catalytic process. The glucose concentration (B) and dissolved O₂ concentration (C) after incubation with different treatments. (D) Masson's trichrome staining of newly formed bone tissues. (E) Immunofluorescence staining against OPN (bone marker), CD31 (vessel marker), CD206 (pro-healing M2 macrophage marker), and iNOS (pro-inflammatory M1 macrophage marker) for evaluating the osteogenic, angiogenic, and anti-inflammatory activity of different 3D printed scaffolds by. Scale bar: 200 μ m (D) and 20 μ m (E). Reprinted (adapted) with permission from ref. 44, copyright 2021, Wiley-VCH.

in blood vessel walls. Currently, statins are the first-line drugs used for treating AS, and they act to reduce plasma lipids by inhibiting the activity of 3-hydroxy-3-methyl-glutaryl coenzyme A reductase. However, only 20–40% of clinical cardiovascular events are reduced, as statins fail to resolve the pathogenesis of AS. The pathogenesis of AS has not been fully elucidated, but high levels of ROS and senescent cells are believed to be closely associated with the AS process. On the one hand, the accumulation of senescent endothelial cells can induce inflammation and oxidative stress to impair endothelial function and stiffen large arteries. In contrast, the antioxidant barrier changes in senescent cells, and antioxidants are exhausted by high levels of ROS, leading to the failure of the antioxidant defense system. During the progression of AS, senescent cells interact with ROS to remodel the pathologic vascular wall and eventually atherosclerosis, demonstrating combined anti-senescence and antioxidant stress as a potential therapeutic intervention for AS therapy. Based on this theory, Wei and colleagues fabricated MOF@Se nanozymes (MSe₁) with antisenescence and antioxidant capacities for application in alleviating AS (Fig. 15A).⁴⁵ The SOD- and GPx-like abilities of the MSe₁ nanozyme are used to sequentially scavenge O₂^{•−} and H₂O₂ through the SOD-GPx

catalytic reactions, therefore inhibiting ROS-induced inflammatory responses in macrophages and human umbilical vein endothelial cells (HUVECs). By protecting DNA from damage, the MSe₁ nanozyme can attenuate HUVEC senescence. Moreover, the MSe₁ nanozyme significantly decreases the cellular uptake of oxidized low-density lipoprotein, thereby suppressing foam cell formation in macrophages and HUVECs. In an apolipoprotein E-deficient mice model, the MSe₁ nanozyme was demonstrated to effectively delay the development of AS (Fig. 15B–D).

3.3 Wound infection management

Wound infections by bacteria are common complaints that have traditionally been treated with antibiotic drugs. However, the widespread use of antibiotics has led to the emergence of multi-drug resistant (MDR) bacteria and new forms of infectious disease. Inspired by natural enzymes that disrupt the structure of cells and interfere with metabolism, Zhou and colleagues developed a manganese-doped dopamine-derived hollow carbon sphere (MnOx/HNCS) nanozyme-triggered cascade catalytic system for the treatment of MDR bacterial infections.⁴⁶ The MnOx/HNCS has multiple enzyme-like activities (OXD-, SOD-, and POD-like activities) under acidic conditions, and

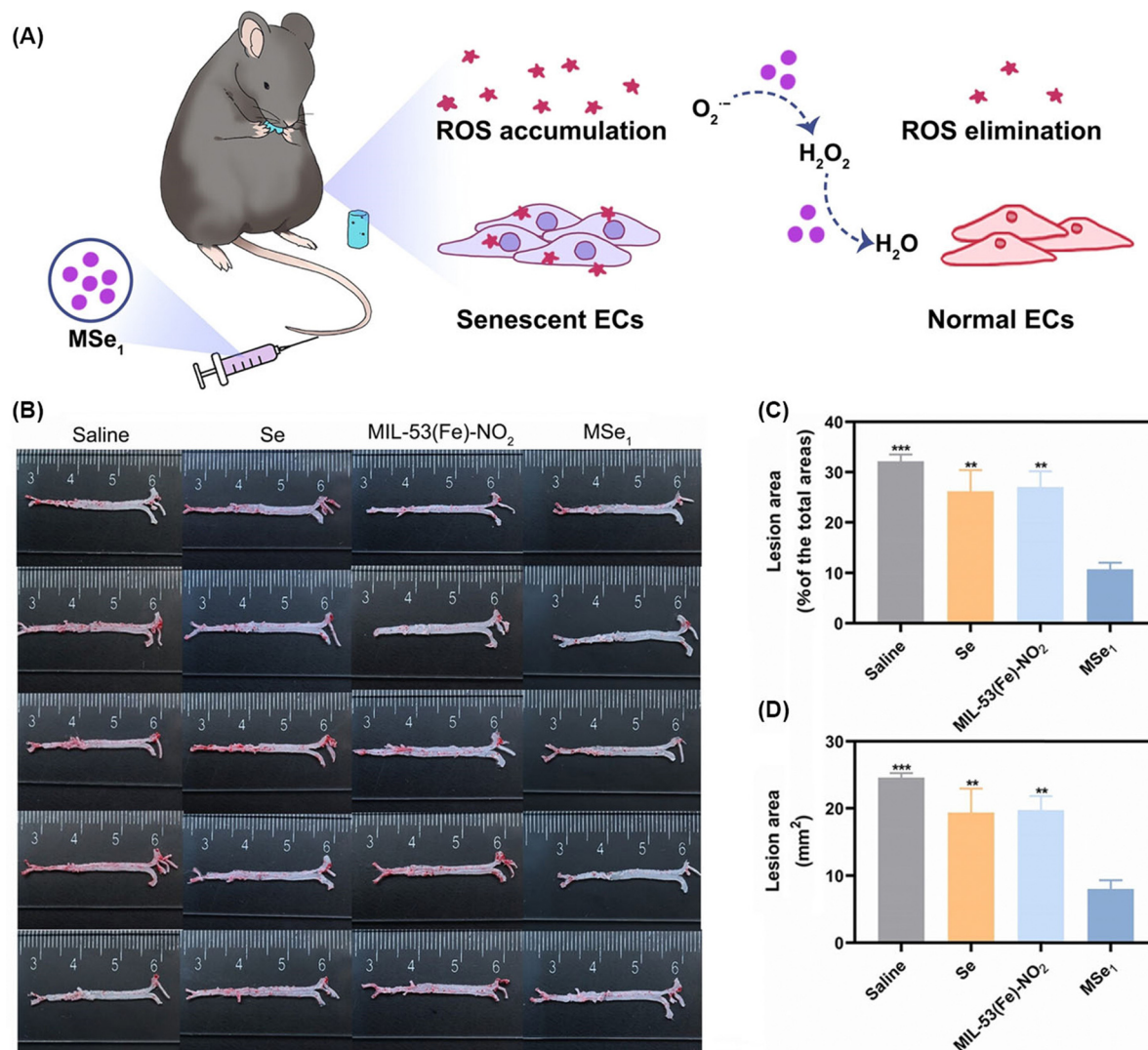


Fig. 15 MSe₁ cascade nanozyme with antisenescence and antioxidant activities for AS therapy. (A) Illustration of MSe₁ nanozyme to scavenge O₂^{•-} via cascade SOD-GPx reactions for treating AS. (B) Photographs of oil red O-stained whole aortas from apolipoprotein E-deficient mice after different nanozymes. Quantitative analysis of the lesion areas of the whole aortas (C) and the lesion area in aortas (D). Data are presented as mean ± SD (*n* = 5). **p* < 0.05, ***p* < 0.01, ****p* < 0.001, and *****p* < 0.0001 vs. MSe₁ group. Reprinted (adapted) with permission from ref. 45, Copyright 2023, Wiley-VCH.

the first to be triggered is its OXD-like activity, which converts O₂ into O₂^{•-}. The SOD-like activity is then used to transform the O₂^{•-} into H₂O₂, which is subsequently converted into •OH by the POD-like activity to kill bacterial cells. Additionally, MnOx/HNCS stimulates the deposition of the extracellular matrix and re-epithelialization to accelerate wound healing. Accordingly, MnOx/HNCS have shown excellent antibacterial efficiency in an MDR bacteria-infected wound mouse model.

Given that biofilm-induced local immune inactivation results in the failure of antibiotics to fight bacterial infections, Liu and colleagues' group developed a ciprofloxacin (Cip) antibiotic-loaded mesoporous nanozyme (HA@MRuO₂-Cip/GOx) containing hyaluronic acid (HA) to overcome bacterial resistance and activate local immunosuppression in the biofilm microenvironment.⁴⁷ The HA controls the enzymatic activities of POD-like MRuO₂ and GOx to minimize damage to normal tissues. After targeting the CD44 protein overexpressed on the

surface of macrophages, the released GOx catalyzes the intracellular glucose to produce H₂O₂. The peroxide then acts as the substrate of the POD-like MRuO₂ to generate •OH, which disrupts biofilms and enhances Cip to kill planktonic bacteria. In addition, HA@MRuO₂-Cip/GOx activates early macrophage-associated host immunity and prevents the recurrence of bacterial chronic lung infections. In a mice bacterial infection model, this nanozyme-mediated cascade catalytic therapy combined with targeted antibiotic delivery could offer an enhanced treatment for bacterial infections with minimal biotoxicity.

Chronic wounds are common complications in diabetic patients, and diabetic wound healing remains challenging when there is continuous glucose accumulation, bacterial infections, hypoxia, and oxidative stress at the wound sites. To modulate the oxidative stress microenvironment in chronic diabetic wounds, Dong and colleagues developed an antioxidative system (MOF/Gel) by integrating a SOD- and CAT-like metal

organic framework (MOF-818) nanzyme with injectable and thermosensitive hydrogels (Gel) for chronic wound healing in diabetic rats (Fig. 16A).⁴⁸ With high levels of SOD- and CAT-like activities, MOF-818 can catalyze the conversion of endogenous $O_2^{\bullet-}$ into O_2 and H_2O_2 , decompose the H_2O_2 into O_2 , and thus significantly relieve oxidative stress. The authors showed that one application of the MOF/Gel achieved wound closure rates comparable to those obtained with clinical drugs that need to be applied every day during the treatment period (Fig. 16B–D). Additionally, Fan and colleagues reported their formulation of a O_2 -supplying glucose-powered cascade catalytic system by anchoring a defect-rich $MoS_2@Au@BSA$ to an injectable hydrogel as an agent that promotes the reconstruction of infected diabetic skin.⁴⁹ The prepared $MoS_2@Au@BSA$ nanzyme exhibits high glucose-activated cascade activity promoted by GOx-like Au, which catalyzes glucose into gluconic acid and H_2O_2 , which is then transformed into $\bullet OH$ via the POD-like activity of the nanzyme for eradicating bacteria in the created acidic microenvironment, therefore accelerating healing. When the wound pH reaches an alkaline condition, the $MoS_2@Au@BSA$ nanzyme converts $O_2^{\bullet-}$ into O_2 and H_2O_2 via its SOD-like activity, and subsequently decomposes excessive H_2O_2 into O_2 via its CAT-like activity, reducing oxidative stress, alleviating hypoxia, and promoting glucose oxidation. When it crosslinked oxidized dextran, and glycol chitosan through a Schiff base, the $MoS_2@Au@BSA$ nanzyme-anchored injectable hydrogel demonstrated excellent self-healing, tissue adhesion, hemostatic, and angiogenic properties, and promoted diabetic wound healing by eradicating bacteria, scavenging ROS, alleviating hypoxia, and facilitating epithelialization, collagen

deposition, and angiogenesis in an *S. aureus*-infected diabetic rat model.

3.4 Other diseases

Hyperuricemia is caused by abnormally high levels of UA in the blood. Some drugs, such as allopurinol and febuxostat, have been used for the treatment of hyperuricemia; however, they only alleviate the symptoms rather than cure the condition. To reduce UA levels for the clinical treatment of hyperuricemia, uricase-based UA degradation medicines that catalyze the conversion of UA into allantoin and H_2O_2 have been approved. However, their extensive application is limited due to the vulnerability of uricase activity and the overproduction of H_2O_2 . To solve these problems, Zheng and colleagues developed a cascade nanoreactor Pd–Ru/uricase@RBC containing RBC membranes for hyperuricemia treatment.²⁰ Pd–Ru/uricase@RBC effectively degrades UA into allantoin and H_2O_2 with uricase, and subsequently employs its CAT-like Pd–Ru activity to catalyze the produced H_2O_2 into H_2O and O_2 . This in turn facilitates the O_2 -dependent catalytic degradation of UA, significantly reducing UA levels. By developing Pd–Ru/uricase@RBC, the authors have potentially realized safe and efficient therapies in a hyperuricemia mouse model. In another notable study, Gao and colleagues designed an artificial peroxisome using a carbon nanzyme with diverse mimicking activity (uricase-, CAT-, POD-, SOD-, and OXD-like activities) that can be used to ameliorate hyperuricemia.⁵⁰ Similarly to Pd–Ru/uricase@RBC, the developed *pero*-nanzyme efficiently reduces UA levels through cyclic cascade reactions mediated by uricase–CAT. With its ability to induce a SOD–CAT cascade, the peroxisome may also be effective as an IS treatment,

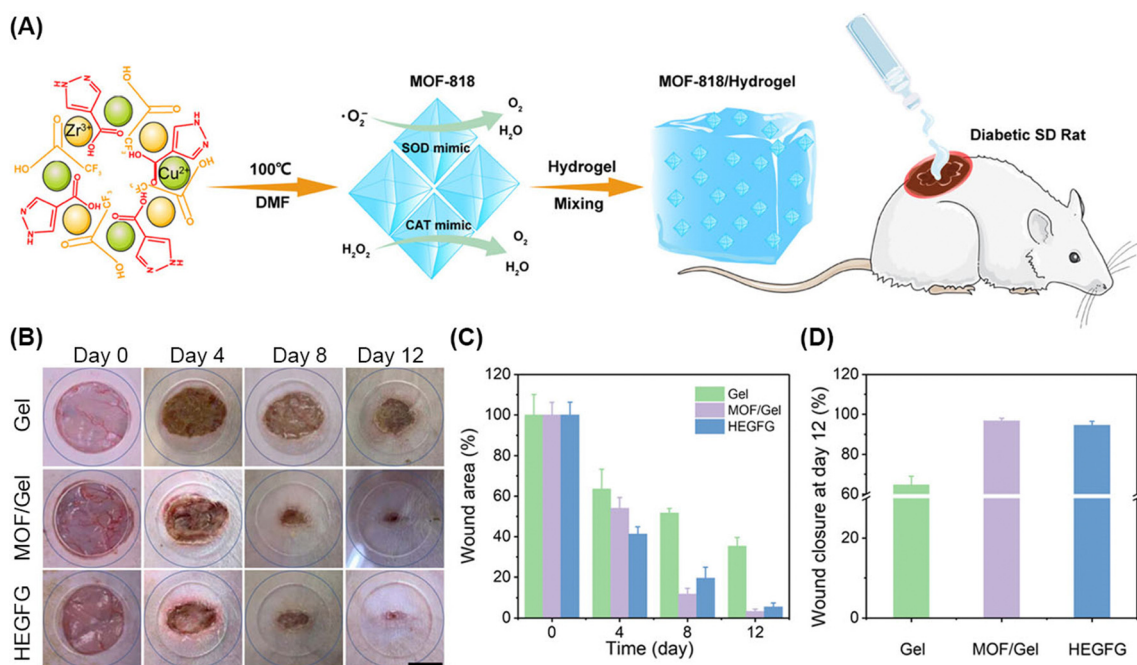


Fig. 16 MOF/Gel antioxidative system for diabetic chronic wound healing. (A) Illustration of the preparation of the MOF/Gel antioxidative system. (B) Photographs of the wounds after different treatments at indicated days. Scale bar: 5 mm. (C) and (D) Quantitative analysis of the wound area at the indicated days. Reprinted (adapted) with permission from ref. 48, Copyright 2022, American Chemical Society.

serving as a promising therapeutic reagent for the management of both hyperuricemia and IS.

Sepsis, a life-threatening disease caused by the deregulation of host immune responses to infections, causes high morbidity and mortality worldwide, which is exasperated by the lack of effective therapies. Evidence suggests that ROS/RNS play a vital role in the pathophysiology of sepsis. Various small molecular antioxidants are available as therapies, such as diethyldithiocarbamate; however, they lack the ability to scavenge multiple ROS/RNS and are unstable under physiological conditions. Due to the good scavenging ability of ROS/RNS under physiological conditions, nanozyme-induced biological cascade reactions have been used for sepsis treatment. For example, Qu and colleagues developed a novel single-atom-enzyme (Co/PMCS),⁵¹ exhibiting SOD-, CAT-, and GPx-like activities, that can efficiently convert $O_2^{\bullet-}$ into O_2 and H_2O_2 via its SOD-like activity. The H_2O_2 is then decomposed into H_2O and O_2 by CAT- and GPx-like activities, respectively. Co/PMCS also exhibits highly effective NO^{\bullet} and $\bullet OH$ scavenging abilities. As such, Co/PMCS was reported to efficiently inhibit proinflammatory cytokine production, leading to improved survival in sepsis mice.

4. Challenges and outlook

In this review, we summarized various enzyme- and/or nanozyme-engineered biocatalytic cascade reactions in disease management.

According to the timeline of catalytic steps, biocatalytic cascade reactions can be classified into five main categories: linear, orthogonal, parallel, cyclic, and triangular cascades. So far, except for the triangular cascades, which have not been reported in disease management, all other cascades have been developed for disease management (Table 2).

With the high catalytic activity and good specificity, enzyme and/or nanozyme-derived biocatalytic cascade nanoreactors can avoid using nontoxic or less toxic nanozymes to react with the intrinsic substrates, which is closely related to the occurrence of diseases. Even after disease management, the residual cascade nanoreactors can still enhance the defense mechanism of the body, facilitating tissue repair and regeneration, and maintaining homeostasis, with the continuing activities of enzymes/nanozymes. Notably, continuous enzyme activity requires monitoring, as excessive or unregulated enzymatic activity can potentially cause unwanted side effects or disrupt normal physiological processes.

After the biocatalytic cascade systems complete their task, the small enzyme fragments or nanozyme particles with appropriate sizes can be excreted in urine. Some can be broken down by the ubiquitous enzymes in the body. For example, proteases can break down proteins and other specific enzymes can target chemical bonds in biocatalytic cascade systems. In addition, some biocatalytic cascade systems may be absorbed and metabolized by liver tissue. The metabolites are then excreted into

Table 2 Summary of biocatalytic cascade systems used for disease management

Cascade catalytic system	Enzyme/enzyme mimic	Cascade categories	Disease type	Ref.
Cu SAzyme	OXD, CAT, POD	Linear cascade	Cancer therapy	24
AFCT nanozyme	SOD, POD, NADH POD	Linear cascade	Cancer theranostics	25
UCNPs@Cu-Cys-GOx	POD, GOx, GSHOx	Orthogonal cascade	Cancer theranostics	26
$Fe_3O_4/Ag/Bi_2MoO_6$	CAT, SOD, POD, GSHOD	Cyclic and orthogonal cascades	Cancer theranostics	16
Ir-N ₅ SA nanozyme	OXD, POD, CAT, NOX	Parallel cascades	Cancer therapy	19
PMNSG	GOx, CAT, POD	Linear and cyclic cascades	Cancer theranostics	27
Co/TiO ₂ SAzyme	CAT, OXD	Linear cascade	Cancer theranostics	28
PHMZCO-AT nanozyme	SOD, POD	Linear cascade	Cancer theranostics	29
O-NZ nanozyme	SOD, GPx	Linear cascade	Traumatic brain injury	10
JCNs	SOD, CAT	Linear cascade	Traumatic brain injury	30
NSC@PCN/HOF	SOD, CAT	Linear cascade	Alzheimer's disease	8
Nb ₂ C MXenzyme	SOD, CAT	Linear cascade	Alzheimer's disease	31
MXenzyme	SOD, CAT, POD, GPx, TPx, HPO	Linear cascade	Parkinson's disease	32
Pt-iNOS@ZIF	SOD, CAT, iNOS	Linear cascade	Hepatic ischemia reperfusion injury	9
$Fe_2NC@Selenium$	SOD, CAT, GPx	Linear cascade	Cerebral ischemia reperfusion injury	33
Mito-fenozyme	SOD, CAT	Linear cascade	Cerebral ischemia reperfusion injury	34
PNzyme/MnO ₂	SOD, CAT	Linear cascade	Reperfusion injury in ischemic stroke	35
$KCa(H_2O)_2[Fe^{III}(CN)_6] \cdot H_2O$	SOD, CAT, POD, GPx	Linear cascade	Acute kidney injury	36
M-TA NMs	SOD, CAT	Linear cascade	Chronic kidney diseases	37
Cu _{5.4} O NPs	SOD, CAT, GPx	Linear cascade	Acute liver/kidney injury, diabetic wound	38
Pt@PCN222-Mn	SOD, CAT	Linear cascade	Crohn's disease and ulcerative colitis	39
LiMn ₂ O ₄	SOD, CAT, GPx	Linear cascade	Ulcerative colitis	40
BL@B-SA ₅₀	SOD, CAT	Linear cascade	Crohn's disease and ulcerative colitis	41
Cu-N ₄ ClG	SOD, CAT	Linear cascade	Osteoarthritis	42
MHPH	Mn-SOD, CAT	Linear cascade	Rheumatoid arthritis	43
Alg/GOx/CaP@CAT	GOx, CAT	Cyclic cascade	Diabetic osteoporosis	44
MSe ₁ nanozyme	SOD, GPx	Linear cascade	Atherosclerosis	45
MnOx/HNCS	OXD, SOD, POD	Linear cascade	Wound infection	46
HA@MRuO ₂ -Cip/GOx	GOx, POD	Linear cascade	Wound infection	47
MOF/Gel	SOD, CAT	Linear cascade	Chronic wound	48
MoS ₂ @Au@BSA	GOx, POD, CAT, SOD	Linear cascade	Chronic wound	49
Pd-Ru/uricase@RBC	Uricase, SOD	Cyclic cascade	Hyperuricemia	19
pero-Nanozysome	Uricase, CAT, POD, SOD, OXD	Linear and cyclic cascades	Hyperuricemia and ischemic stroke	50
Co/PMCS	SOD, CAT, GPx	Linear cascade	Sepsis	51

the bile and eliminated through the gastrointestinal tract. Meanwhile, enzymes in the liver can also break down enzymes and other molecules from the biocatalytic cascade systems, and convert them into small molecules that can be absorbed or excreted. In addition, the immune system can recognize foreign enzymes and nanozymes as antigens, facilitating their clearance by immune cells. In short, the body has multiple mechanisms to eliminate the enzymes/nanozymes.

Despite great progress being made in the design and application of biocatalytic cascade systems for disease management, they still face many challenges to be addressed in the future.

(1) Construction of biocatalytic cascade systems. Currently, only a limited number of enzyme-derived biocatalytic cascade systems have been reported, and most biocatalytic cascade systems are engineered by multiple nanozymes or a single nanozyme with multienzyme-like activities. In the case of natural enzymes-engineered cascade systems, they encounter inherent challenges, such as low operational stability, short shelf life, and the need for mild catalytic conditions. To overcome these challenges, AlphaFold and protein engineering including site-directed mutagenesis techniques and directed evolution methods can be used in combination to rapidly generate enzyme mutants with improved stability against pH and temperature variation. Besides, high-throughput screening technology can be used to quickly screen out enzymes and reaction conditions (such as pH, temperature, substrate specificity, *etc.*) with optimized catalytic efficiency from a large number of enzymes and reaction condition combinations. For example, using gene library construction, microfluidic chip and other technologies can screen thousands or even tens of thousands of different enzymes or reaction conditions, facilitating the design of efficient biocatalytic cascade systems. Moreover, computational chemistry, molecular dynamics simulation and other methods should be used to theoretically simulate and predict the process of biocatalytic cascade reactions. By calculating the interaction between substrates and enzymes, energy changes of reactions, formation and conversion of intermediate products, *etc.*, the mechanism of cascade reactions can be deeply understood, providing theoretical guidance for the design of biocatalytic cascade systems. Furthermore, carriers are crucial for efficient delivery of multiple enzymes to organs/cells, and biodegradable organic polymers represent a promising alternative to encapsulate enzymes as they can provide a relatively stable microenvironment and protect them from external adverse factors, such as organic solvents, extreme pH conditions, *etc.*

In addition, nanozymes with tunable catalytic activity can also serve as carriers for natural enzymes. The nanozyme-enzyme cascade nanoreactors exhibit good catalytic stability and high efficiency. To improve catalytic selectivity, combining recognition mechanisms such as creating protein-like binding pockets and molecular imprinting of selective substrate pockets would provide promising approaches to develop nanozymes with high specificity. If possible, it would be better to build a database for the relationships between the structure of nanozymes and the catalytic performance. As such, the nanozymes

with desired functions can be synthesized more easily, similar to the synthesis of enzyme proteins in living systems. Besides, similar to enzyme-engineered cascade systems, carriers are crucial for nanozyme-enzyme cascade nanoreactors, and biodegradable organic polymers are also a promising alternative. In addition, there are several factors that should be considered in the design of nanozyme-enzyme cascade systems, including the difference in reaction rate between nanozymes and enzymes, the complex reaction environment, the inhibitory effect of intermediate products or by-products on the enzymes, and the possible catalytic interference of nanozymes due to its multi-enzymatic activities.

In the case of some nanozymes, they possess multi-enzymatic activities and have demonstrated great potential of cascade catalytic therapy in small animals (mice). However, they have several drawbacks such as the difficulty of precisely regulating enzymatic activities, the reduced specificity, the complexity of safety and biocompatibility issues, and difficulties in characterization and quality control. To precisely regulate multi-enzymatic activities, nanozymes with core-shell, porous, or Janus structures represent promising alternatives as they can provide different active sites within a single nanostructure, enabling more independent control of their activities. Additionally, the strategy of mimicking the active site and structure of natural enzymes provides great potential in improving the selectivity and activity of nanozymes. Furthermore, through computational methods such as molecular dynamic simulations, the activities of nanozymes under different conditions can be predicted. The interactions between active sites, the effect of different regulators, and the response to environmental changes can be modeled. For instance, simulations can predict how a change in the distance between two active sites will affect their activities. Based on the computational results, the optimal parameters, including the regulators concentration, the time of exposure to a particular stimulus, and the sequence of regulatory steps for activity regulation, can be determined, thus more precise control of the multi-enzymatic activities of nanozymes can be achieved. Besides, artificial intelligence techniques can be employed to design suitable nanozymes for cascade catalytic therapy.

(2) To improve the accumulation of biocatalytic cascade systems at the lesion sites. It is challenging to target specific tissues and cells, as the biological environment within living organisms is heterogeneous, and different cells possess distinct characteristics and microenvironments. For the accumulation of biocatalytic cascade systems, passive, active, or endogenous targeting modes either separately or in combination can be explored to achieve the desired accumulation. Passive targeting relies on the physical properties of biocatalytic cascade systems, such as size, shape, surface charge, stiffness, *etc.*, to interact with anatomy and physiology. Active targeting involves surface modification with a chemical or biological moiety, which enables the systems to specifically bind to receptors or other cellular features highly expressed by cells within a target organ. Endogenous targeting entails engineering the composition of a system so that it binds to specific plasma proteins during circulation. These plasma proteins then direct the system to the target organ and

facilitate their uptake by specific cells. Current studies mainly focus on passive and active targeting strategies. An endogenous targeting strategy is also worth studying to improve the accumulation of biocatalytic cascade systems at the lesion sites. In addition, the route of administration is another determinant of *in vivo* biodistribution. Different administration routes, such as inhalation, intratumoral, intravenous, intranodal, subcutaneous, and intramuscular, can be used for the administration of biocatalytic cascade systems, which can directly affect the *in vivo* pharmacokinetics and biodistribution.

(3) Mechanistic evaluation of biocatalytic cascade reactions in disease management. A comprehensive understanding of the mechanisms underlying disease treatment is crucial for the development of application-oriented biocatalytic cascade systems. Currently, a lot of biocatalytic cascade systems have demonstrated good therapeutic efficacy in small animals (mice). However, monitoring the cascade reaction kinetics *in vivo* is a big challenge as the existing information can only support the therapeutic outcome rather than the process. With the development of multifunctional probes capable of detecting the concentration and distribution of specific biochemicals in the biological environment, it is expected that these diagnostic agents can be useful in monitoring the catalytic process *in vivo* and clarifying the relationship between the structure and/or composition of cascade systems and *in vivo* performance. With well-defined catalytic mechanisms, biocatalytic cascade systems can be designed for personalized disease management.

(4) Development of application-oriented biocatalytic cascade systems. In disease treatment, targeting activation of cascade nanoreactors can not only avoid unnecessary and even harmful catalytic reactions in organisms but also enhance the efficiency of catalytic therapy. For instance, cascade nanoreactor-mediated ROS amplification can not only be used for anticancer therapy, but can also influence the metabolism of surrounding immune cells, thus reducing the therapeutic effect. To achieve application-oriented catalytic therapy, biocatalytic cascade systems can be designed to be activated in specific microenvironments, such as acidity and hypoxia in bacterial infection microenvironments and tumor tissues, ion dyshomeostasis in neurodegenerative microenvironments, and high levels of ROS in acute liver/kidney injury. Additionally, different subcellular localizations have distinct specific metabolic pathways. Thus, biocatalytic cascade systems can also be developed to precisely target specific metabolic pathways to improve their therapeutic efficiency.

(5) Systematic evaluation on the biosafety of biocatalytic cascade systems. For biomedical applications, the *in vivo* dynamics and ultimate fates of these systems should be systematically investigated at different treatment stages, including stability, pharmacokinetics, distribution, metabolism, duration of therapeutic effect, excretion, and toxicity. Current studies primarily focus on their therapeutic outcomes, yet the impact on the complex metabolic network remains unelucidated, and the *in vivo* biosafety requires further exploration. On the one hand, most nanozymes are inorganic metal oxides (such as Fe_3O_4 , TiO_2 , etc.), which may cause long-term potential toxicity,

as metal ions may be released after their biodegradation, thus interfering with the ion balance within cells, resulting in metal dyshomeostasis accompanied by side effects. Moreover, the release of metal ions may cause damage to organs like the liver and kidneys since these organs are crucial organs for metabolism and excretion. Metal-free nanoreactors could offer possible solutions to overcome this concern. On the other hand, biocatalytic cascade systems may trigger an immune response, leading to inflammation. The prolonged exposure of cascade systems may lead to the development of immune tolerance, where the immune system becomes less responsive over time. Therefore, the long-term effects, underlying biological toxicity, and immunogenicity should be fully evaluated. Additionally, to develop biocompatible and environment-friendly biocatalytic cascade systems, effective theoretical and statistical models should be established.

(6) The bottleneck of clinical application. Biocatalytic cascade reactions have great promise in disease treatment. However, there are several major bottlenecks in clinical application. Firstly, both therapeutic enzymes and nanozymes encounter the stability challenge. In the case of therapeutic enzymes, they have the problems of temperature stability, pH stability, and sensitivity to proteases. Temperature stability not only impacts storage and transportation but also influences the therapeutic effect within patients. Additionally, different tissues and organs in the human body have diverse pH environments. For instance, the stomach is an acidic environment with a pH ranging from around 1.5 to 3.5, while the blood pH is approximately 7.35 to 7.45. Natural enzymes typically remain stable and active only within a specific pH range, making it difficult to maintain the optimal pH condition for enzymatic reactions. Although nanozymes have certain advantages in stability compared to natural enzymes, their activities may also decline under long-term storage or *in vivo* conditions. For example, the activity of some nanozymes may be affected by factors such as the adsorption of biomolecules in the body and the redox environment. Second, cascade catalysts raise biocompatibility concerns. Natural enzymes from non-human sources and nanozymes can trigger immune responses. Once introduced into the body, the immune system may recognize them as foreign antigens and generate antibodies against them, thereby resulting in adverse effects, such as inflammation, allergic reactions, and the rapid clearance of enzymes/nanozymes from the body. Third, it is challenging to control the selectivity of cascade reactions in the body since regulating cascade reactions *in vivo* is a complex task. In a laboratory environment, reaction conditions such as temperature and substrate concentrations can be precisely controlled. However, in the human body, these factors are much more difficult to manage. There is a need for better strategies to turn cascade reactions on and off to optimize the therapeutic effect and minimize side effects. Fourth, both enzymes and nanozymes encounter difficulties in target delivery. Whether natural enzymes or nanozymes, they all need to be specifically delivered to the disease sites. However, current delivery systems often struggle to achieve precise targeting, leading to non-specific distribution. This not only diminishes the therapeutic effect but may also cause side effects. Therefore, it is essential to develop

specific targeting mechanisms. Fifth, there is a lack of methods to monitor the cascade catalytic reactions in real-time during clinical treatment. Understanding the progress of cascade reactions, such as the degree of substrate conversion and enzymatic activity, is of crucial importance for evaluating the efficacy of treatment. Current imaging techniques may not be sensitive enough for specific cascade reactions. Additionally, visualizing the distribution of enzymes/nanozymes and substrates in the body also poses a challenge. Without accurate visualization methods, it is difficult to adjust the treatment plan to optimize the delivery and activity of cascade catalytic systems. Finally, obtaining regulatory approval is difficult as regulators need to thoroughly assess its potential risks. Biocatalytic cascade systems involve new biomaterials and treatment technologies, so the regulatory approval process is relatively complex. It is necessary to meet strict safety, effectiveness, and quality control standards, which increases the difficulty and time cost for their entry into clinical applications. In short, biocatalytic cascade reactions exhibit promising potential in the management of various diseases. Further studies focusing on overcoming these challenges will significantly contribute to the field of precision medicine.

Data availability

No new data were created or analysed during this study. Data sharing is not applicable to this article.

Conflicts of interest

There are no conflicts to declare.

Acknowledgements

This work is financially supported by the National Key R&D Program of China (2020YFA0908800), the National Natural Science Foundation of China (82071985, U23A2097, 82372116, 32301201, 22104094, 82441015, 22474079), the Basic Research Program of Guangdong (2024A1515012677), the Shenzhen Medical Research Fund (B2302047), the Shenzhen Science and Technology Program (JCYJ20220818095806014, KQTD20190929172538530, JCYJ20240813142810014), and the Research Team Cultivation Program of Shenzhen University (2023QNT017, 2023QNT019).

Notes and references

- 1 D. C. Miller, S. V. Athavale and F. H. Arnold, *Nat. Synth.*, 2022, **1**, 18–23.
- 2 K. Chen and F. H. Arnold, *Nat. Catal.*, 2020, **3**, 203–213.
- 3 M. Vázquez-González, C. Wang and I. Willner, *Nat. Catal.*, 2020, **3**, 256–273.
- 4 B. Yang, Y. Chen and J. Shi, *Adv. Mater.*, 2019, **31**, 1901778.
- 5 D. Jiang, D. Ni, Z. T. Rosenkrans, P. Huang, X. Yan and W. Cai, *Chem. Soc. Rev.*, 2019, **48**, 3683–3704.
- 6 X. Zhang, G. Li, G. Chen, D. Wu, Y. Wu and T. D. James, *Adv. Funct. Mater.*, 2021, **31**, 2106139.
- 7 A. I. Benítez-Mateos, D. Roura Padrosa and F. Paradisi, *Nat. Chem.*, 2022, **14**, 489–499.
- 8 D. Yu, H. Zhang, Z. Liu, C. Liu, X. Du, J. Ren and X. Qu, *Angew. Chem., Int. Ed.*, 2022, **61**, e202201485.
- 9 J. Mu, C. Li, Y. Shi, G. Liu, J. Zou, D.-Y. Zhang, C. Jiang, X. Wang, L. He, P. Huang, Y. Yin and X. Chen, *Nat. Commun.*, 2022, **13**, 2513.
- 10 X. Mu, J. Wang, H. He, Q. Li, B. Yang, J. Wang, H. Liu, Y. Gao, L. Ouyang, S. Sun, Q. Ren, X. Shi, W. Hao, Q. Fei, J. Yang, L. Li, R. Vest, T. Wyss-Coray, J. Luo and X.-D. Zhang, *Sci. Adv.*, 2021, **7**, eabk1210.
- 11 C. Wu, L. Qin, D. Niu, X. Wang, Q. Zhang, Y. Shang, M. Hu, X. Han, S. Shen, X. Qin, S. Xi, Y. Li and Q. Wang, *Adv. Funct. Mater.*, 2021, **31**, 2103531.
- 12 L. Zhang, Q.-C. Yang, S. Wang, Y. Xiao, S.-C. Wan, H. Deng and Z.-J. Sun, *Adv. Mater.*, 2022, **34**, 2108174.
- 13 J. Liu, A. Wang, S. Liu, R. Yang, L. Wang, F. Gao, H. Zhou, X. Yu, J. Liu and C. Chen, *Angew. Chem., Int. Ed.*, 2021, **60**, 25328–25338.
- 14 G. Zhou and M. Li, *Adv. Mater.*, 2022, **34**, 2200871.
- 15 Y. Sheng, I. A. Abreu, D. E. Cabelli, M. J. Maroney, A.-F. Miller, M. Teixeira and J. S. Valentine, *Chem. Rev.*, 2014, **114**, 3854–3918.
- 16 C. Cao, H. Zou, N. Yang, H. Li, Y. Cai, X. Song, J. Shao, P. Chen, X. Mou, W. Wang and X. Dong, *Adv. Mater.*, 2021, **33**, 2106996.
- 17 J. Xiao, L. Hai, Y. Li, H. Li, M. Gong, Z. Wang, Z. Tang, L. Deng and D. He, *Small*, 2022, **18**, 2105465.
- 18 W. Zhen, Y. Liu, W. Wang, M. Zhang, W. Hu, X. Jia, C. Wang and X. Jiang, *Angew. Chem., Int. Ed.*, 2020, **59**, 9491–9497.
- 19 Y. Liu, B. Wang, J. Zhu, X. Xu, B. Zhou and Y. Yang, *Adv. Mater.*, 2023, **35**, 2208512.
- 20 J. Ming, T. Zhu, J. Li, Z. Ye, C. Shi, Z. Guo, J. Wang, X. Chen and N. Zheng, *Small*, 2021, **17**, 2103645.
- 21 S. Zhang, Y. Zhang, Y. Feng, J. Wu, Y. Hu, L. Lin, C. Xu, J. Chen, Z. Tang, H. Tian and X. Chen, *Adv. Mater.*, 2022, **34**, 2206851.
- 22 Y.-P. Xiao, P.-H. Chen, S. Lei, F. Bai, L.-H. Fu, J. Lin and P. Huang, *Angew. Chem., Int. Ed.*, 2022, **61**, e202204584.
- 23 B. Yu, W. Wang, W. Sun, C. Jiang and L. Lu, *J. Am. Chem. Soc.*, 2021, **143**, 8855–8865.
- 24 M. Chang, Z. Hou, M. Wang, D. Wen, C. Li, Y. Liu, Y. Zhao and J. Lin, *Angew. Chem., Int. Ed.*, 2022, **61**, e202209245.
- 25 S. Dong, Y. Dong, Z. Zhao, J. Liu, S. Liu, L. Feng, F. He, S. Gai, Y. Xie and P. Yang, *J. Am. Chem. Soc.*, 2023, **145**, 9488–9507.
- 26 M. Wang, M. Chang, C. Li, Q. Chen, Z. Hou, B. Xing and J. Lin, *Adv. Mater.*, 2022, **34**, 2106010.
- 27 S. Lei, J. Zhang, N. T. Blum, M. Li, D.-Y. Zhang, W. Yin, F. Zhao, J. Lin and P. Huang, *Nat. Commun.*, 2022, **13**, 1298.
- 28 H. Wang, Y. Wang, L. Lu, Q. Ma, R. Feng, S. Xu, T. D. James and L. Wang, *Adv. Funct. Mater.*, 2022, **32**, 2200331.
- 29 S. Dong, Y. Dong, B. Liu, J. Liu, S. Liu, Z. Zhao, W. Li, B. Tian, R. Zhao, F. He, S. Gai, Y. Xie, P. Yang and Y. Zhao, *Adv. Mater.*, 2022, **34**, 2107054.

- 30 H. Wang, X. Chen, Y. Qi, C. Wang, L. Huang, R. Wang, J. Li, X. Xu, Y. Zhou, Y. Liu and X. Xue, *Adv. Mater.*, 2022, **34**, 2206779.
- 31 C. Du, W. Feng, X. Dai, J. Wang, D. Geng, X. Li, Y. Chen and J. Zhang, *Small*, 2022, **18**, 2203031.
- 32 W. Feng, X. Han, H. Hu, M. Chang, L. Ding, H. Xiang, Y. Chen and Y. Li, *Nat. Commun.*, 2021, **12**, 2203.
- 33 R. Tian, H. Ma, W. Ye, Y. Li, S. Wang, Z. Zhang, S. Liu, M. Zang, J. Hou, J. Xu, Q. Luo, H. Sun, F. Bai, Y. Yang and J. Liu, *Adv. Funct. Mater.*, 2022, **32**, 2204025.
- 34 Y. Zhang, A. Khalique, X. Du, Z. Gao, J. Wu, X. Zhang, R. Zhang, Z. Sun, Q. Liu, Z. Xu, A. C. Midgley, L. Wang, X. Yan, J. Zhuang, D. Kong and X. Huang, *Adv. Mater.*, 2021, **33**, 2006570.
- 35 Z. Wang, Y. Zhao, Y. Hou, G. Tang, R. Zhang, Y. Yang, X. Yan and K. Fan, *Adv. Mater.*, 2024, **36**, 2210144.
- 36 K. Wang, Y. Zhang, W. Mao, W. Feng, S. Lu, J. Wan, X. Song, Y. Chen and B. Peng, *Adv. Funct. Mater.*, 2022, **32**, 2109221.
- 37 Z. Wei, G. Peng, Y. Zhao, S. Chen, R. Wang, H. Mao, Y. Xie and C. Zhao, *ACS Nano*, 2022, **16**, 18329–18343.
- 38 T. Liu, B. Xiao, F. Xiang, J. Tan, Z. Chen, X. Zhang, C. Wu, Z. Mao, G. Luo, X. Chen and J. Deng, *Nat. Commun.*, 2020, **11**, 2788.
- 39 Y. Liu, Y. Cheng, H. Zhang, M. Zhou, Y. Yu, S. Lin, B. Jiang, X. Zhao, L. Miao, C.-W. Wei, Q. Liu, Y.-W. Lin, Y. Du, C. J. Butch and H. Wei, *Sci. Adv.*, 2020, **6**, eabb2695.
- 40 Q. Wang, C. Cheng, S. Zhao, Q. Liu, Y. Zhang, W. Liu, X. Zhao, H. Zhang, J. Pu, S. Zhang, H. Zhang, Y. Du and H. Wei, *Angew. Chem., Int. Ed.*, 2022, **61**, e202201101.
- 41 F. Cao, L. Jin, Y. Gao, Y. Ding, H. Wen, Z. Qian, C. Zhang, L. Hong, H. Yang, J. Zhang, Z. Tong, W. Wang, X. Chen and Z. Mao, *Nat. Nanotechnol.*, 2023, **18**, 617–627.
- 42 J. Zhong, X. Yang, S. Gao, J. Luo, J. Xiang, G. Li, Y. Liang, L. Tang, C. Qian, J. Zhou, L. Zheng, K. Zhang and J. Zhao, *Adv. Funct. Mater.*, 2023, **33**, 2209399.
- 43 B. Yang, H. Yao, J. Yang, C. Chen, Y. Guo, H. Fu and J. Shi, *J. Am. Chem. Soc.*, 2022, **144**, 314–330.
- 44 C. Yang, Z. Zheng, M. R. Younis, C. Dong, Y. Chen, S. Lei, D.-Y. Zhang, J. Wu, X. Wu, J. Lin, X. Wang and P. Huang, *Adv. Funct. Mater.*, 2021, **31**, 2101372.
- 45 W. Liu, Y. Zhang, G. Wei, M. Zhang, T. Li, Q. Liu, Z. Zhou, Y. Du and H. Wei, *Angew. Chem., Int. Ed.*, 2023, **62**, e202304465.
- 46 M. Lu, S. Li, X. Xiong, Z. Huang, B. Xu, Y. Liu, Q. Wu, N. Wu, H. Liu and D. Zhou, *Adv. Funct. Mater.*, 2022, **32**, 2208061.
- 47 X. Zhu, J. Guo, Y. Yang and J. Liu, *Small*, 2023, **19**, 2204928.
- 48 D. Chao, Q. Dong, Z. Yu, D. Qi, M. Li, L. Xu, L. Liu, Y. Fang and S. Dong, *J. Am. Chem. Soc.*, 2022, **144**, 23438–23447.
- 49 Y. Li, R. Fu, Z. Duan, C. Zhu and D. Fan, *Small*, 2022, **18**, 2200165.
- 50 J. Xi, R. Zhang, L. Wang, W. Xu, Q. Liang, J. Li, J. Jiang, Y. Yang, X. Yan, K. Fan and L. Gao, *Adv. Funct. Mater.*, 2021, **31**, 2007130.
- 51 F. Cao, L. Zhang, Y. You, L. Zheng, J. Ren and X. Qu, *Angew. Chem., Int. Ed.*, 2020, **59**, 5108–5115.